Biosensors and Bioelectronics 136 (2019) 60–75

Contents lists available at ScienceDirect

Biosensors and Bioelectronics

journal homepage: www.elsevier.com/locate/bios

Signal amplification strategies for paper-based analytical devices

Linyang Liu[a,b], Danting Yang[a,b,c], Guozhen Liu[a,b,d,*]

[a] Graduate School of Biomedical Engineering, ARC Centre of Excellence in Nanoscale Biophotonics (CNBP), Faculty of Engineering, The University of New South Wales, Sydney, 2052, Australia
[b] Australian Centre for NanoMedicine, The University of New South Wales, Sydney, 2052, Australia
[c] Department of Preventative Medicine, Medical School of Ningbo University, Ningbo, 315211, PR, China
[d] International Joint Research Center for Intelligent Biosensor Technology and Health, Central China Normal University, Wuhan, 430079, PR, China

ARTICLE INFO

Keywords:
Paper-based analytical devices
Signal amplification
Lateral flow assays
Nanomaterials
Microfluidics
Nucleic acid amplifications

ABSTRACT

Paper-based analytical devices (PADs) are very popular for point-of-care diagnostics, which provide a fast, cost-effective and possible multiplexed detection of a spectrum of molecules. They have been matching forward proudly to contribute to the modern analytical science and life science. Accompanying with their advantages and huge potentials, low detection sensitivity is continuing to challenge the application of PADs from bench to bedside. In order to improve the sensitivity and enhance the signal readout, variable signal amplification strategies have been investigated and applied for PADs. In this review, we have firstly classified formats of PADs according to the engineering design. Advances for improving sensitivity of PADs in recent five years are then summarised according to three popular types of signal amplification strategies (nanomaterial based, nucleic acid based, and engineering of PADs based). Pros and cons of each signal amplification approach have been discussed accordingly. Finally, the future perspectives of PADs are proposed.

1. Introduction

1.1. Point-of-care (POC) diagnostics and paper-based analytical devices (PADs)

Diagnostics plays an important role in the healthcare realm. The reliability and accuracy of diagnostics have great impact on clinical decision-making, treatment and the patient survival rate (Sharma et al., 2015). Infectious diseases such as immunodeficiency syndrome (AIDS) and tuberculosis (TB) and different types of cancer cause a huge burden to economy especially in developing countries due to the low survival rate and the cause of disability. Additionally, the lack of laboratories and modern equipment make it difficult for patients in rural area to be treated quickly and wisely (Hu et al., 2014; Peeling and Mabey, 2010). The modern diagnostic technologies such as polymerase chain reaction (PCR) and enzyme-linked immunosorbent assay (ELISA) *etc.* require trained personnel and expensive instruments, which are not suitable for point-of-care (POC) diagnostics especially in resources limited settings. POC diagnostic technologies meet the ASSURED criteria recommended by World Health Organization (WHO), which is affordable, sensitive, specific, user-friendly, rapid and robust, equipment-free and deliverable to end-users (Choi et al., 2017a). Besides applications in healthcare, POC testings are utilized in other areas, such as biosecurity, environmental and food safety (Sajid et al., 2015; Wu et al., 2017). The global market of POC diagnostics was valued at USD 23.71 Billion in 2017 and is estimated to reach USD 38.13 Billion by 2022 with a compound annual growth rate (CAGR) of 10% during the forecast period (PRNewswire, 2018).

Since the first paper-based microfluidic was rediscovered as a promising analytical platform by Whiteside's research group in 2007 (Martinez et al., 2007), PADs, such as lateral flow assays, dipstick assays, and microfluidic PADs (μPADs) are emerging as promising lightweight, disposable and cost-effective formats, especially for developing countries and POC testing (Mahato et al., 2017). Number of publications on POC devices and PADs since 2013 has been increasing while PADs represent the majority portion of POC devices each year (Fig. 1). Although PADs have achieved highly active academic developments, their entry into real-life applications is still very limited due to several challenges such as low sensitivity and specificity, limited stability and possible requirement of associated equipment, which has been recently summarised in a review (Yamada et al., 2017). Among these challenges, low sensitivity is a significant bottleneck associated with PADs. In this review, we focus on summarising and discussing signal amplification strategies applied to PADs in last five years to enhance the sensitivity of

* Corresponding author. Graduate School of Biomedical Engineering, ARC Centre of Excellence in Nanoscale Biophotonics (CNBP), Faculty of Engineering, The University of New South Wales, Sydney, 2052, Australia
E-mail address: guozhen.liu@unsw.edu.au (G. Liu).

https://doi.org/10.1016/j.bios.2019.04.043
Received 18 March 2019; Received in revised form 15 April 2019; Accepted 21 April 2019
Available online 24 April 2019
0956-5663/

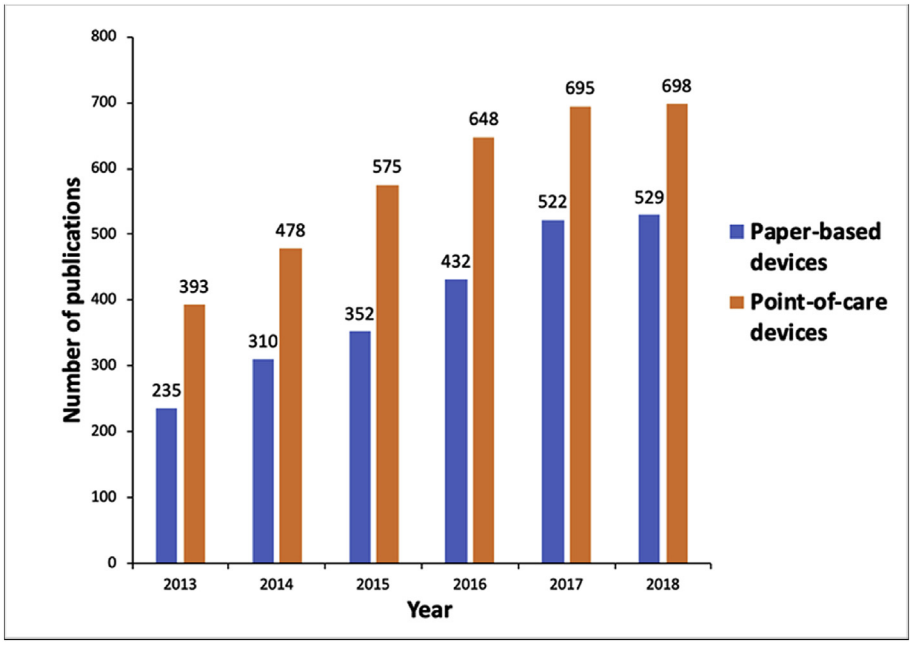

Fig. 1. Annual trends in the number of publications for paper-based devices (blue) and point-of-care devices (orange) from 2013 to 2018. Data obtained from Web of Science. Database selected as: Web of Science Core Collection. (For interpretation of the references to color in this figure legend, the reader is referred to the Web version of this article.)

PADs.

1.2. Classification of PADs and their detection methods

Different signal readout methods have been used on PADs including colorimetry (Lathwal and Sikes, 2016; Ye and Xia, 2018), conductivity (Li et al. 2014a, 2014c), fluorescence (Deng et al., 2018; You et al., 2017), electrochemistry (EC) (Li et al., 2014b; Ma et al., 2015), chemiluminescence (CL) (Park et al., 2015; Zangheri et al., 2015), electrochemiluminescence (ECL) (Liu et al., 2014c; Wang et al., 2013a) and surface-enhanced Raman spectroscopy (SERS) (Chen et al., 2016a; Hasanzadeh and Shadjou, 2016). These signals can be reported by unaided eyes, smartphones, microscopy with cameras coupled with image analysis software et al. No matter what signal readout strategy is used on PADs, there are three classifications of PADs such as dipsticks assays, lateral flow assays and μPADs (Hu et al., 2014), which will be described respectively in the below sections, along with their advantages and limitations in POC diagnostics.

1.2.1. Dipstick assays

The dipstick assays are the simplest PADs, for example, the pH strips (Fig. 2A). The only detection method of dipstick assays is colorimetric done by unaided eyes (Parolo and Merkoci, 2013). Additionally, urine dipsticks are routinely performed to diagnose individual health conditions such as diabetes, kidney disease, and hydration state, which allow screening those multiple disorders by simply dipping a plastic-backed testing paper pad with chromogens into an untreated urine specimen (Yamada et al., 2017). Relevant products have been launched by multiple companies such as Roche Diagnostics, YD Diagnostics, Siemens Healthcare GmBH (Yamada et al., 2017), suggesting the great advantages of dipstick assays in commercial applications.

1.2.2. Lateral flow assays (LFAs)

LFAs (Fig. 2B) are another popular type of PADs used in environmental analysis, food safety and medical diagnostics areas providing rapid, simultaneous and multiplexed detection of different analytes, for example, cancer biomarkers, nucleic acids, heavy metals, microorganisms *etc.* (Koczula and Gallotta, 2016) LFAs generally compose of four different parts: sample pad, on which the sample should be added; conjugation pad, on which the labelled tags conjugate to the biorecognition elements; nitrocellulose membrane which contains test line and control line for reactions; absorbent pad, which reserves excess reagents and prevents backflow (Fig. 2B) (Bahadır and Sezgintürk, 2016). According to the difference in bio-recognition molecules such as antibodies or oligonucleotides (aptamers), LFAs can be characterized into two different categories (antibody-based LFAs (lateral flow immunoassays (LFIAs) (Koczula and Gallotta, 2016)) and aptamer-based LFAs (Cao et al., 2018)). So far pregnancy test strips are the most successful LFAs reaching commercialisation for POC diagnostics.

1.2.3. μPADs

Microfluidic devices have been achieving big success in POC diagnostics because of their adaptable capability with various functional units such as pumps, reactors and valves, and to be integrated into a miniaturized analytical system for further analysis, as well as easy integration with paper surface to form μPADs (Hu et al., 2014). The hydrophilic and hydrophobic microchannel networks of μPADs enable fluid handling in small volumes and quantitative analysis in healthcare, medicine and other diagnostics areas (Xia et al., 2016b). The fluid movement in most of μPADs is driven by capillary forces, and generally, there are two μPAD structures (two-dimensional (2D) and three-dimensional (3D) structures). The microchannels of 2D μPADs (Fig. 2C) are formed by patterning chemical or physical hydrophobic barriers on paper (Hu et al., 2014) using different methods such as wax printing (Xia et al., 2016b), photolithography (Yu and Shi, 2015), inkjet printing (Yamada et al., 2015), screen printing (Lamas-Ardisana et al., 2017) et al. While 3D μPADs (Fig. 2D) are generally fabricated by stacking layers of paper which enables connections between channels in adjacent layers (Hu et al., 2014). Origami, a term for paper folding, is widely used for building up the 3D structures achieving a high degree of folding (Hasanzadeh and Shadjou, 2016). Instead of taping the individual sheet of μPADs together, the origami PADs are fabricated by folding the patterned paper, and using a pre-fabricated clamp or lamination process to hold the structure together (Yetisen et al., 2013). Origami PADs provide platforms for signal amplification methods and are often used for colorimetric (Liu and Crooks, 2011), fluorescence (Xu et al., 2016), electrochemical (Li et al. 2014a, 2014b, 2014c, 2014d; Liu et al. 2012, 2014a; Ma et al., 2015; Sun et al., 2014; Wu et al., 2014a), electrochemiluminescent (Wang et al., 2013a; Wu et al., 2015a), and photoelectrochemical (Ge et al., 2015; Wang et al., 2013b) detections. Unfortunately, currently there is no commercialized product based on μPAD due to the challenges associated with the flow control (Akyazi

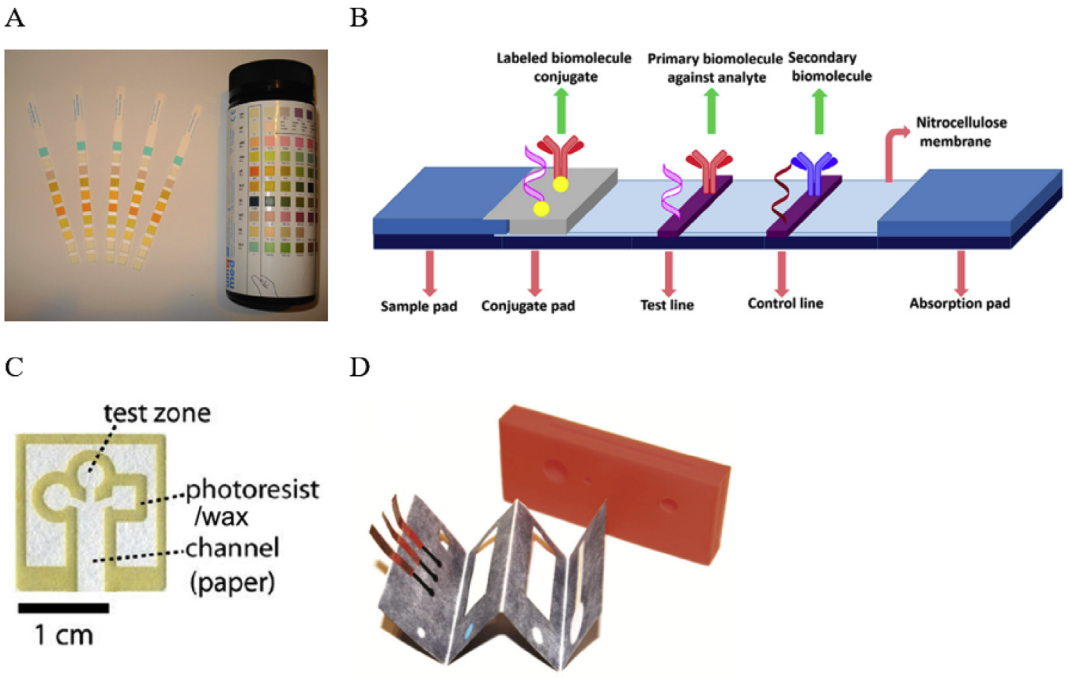

Fig. 2. Different types of PADs. A: Photo of dipstick assays. Reprinted with permission from (Hu et al., 2014). B: The structure of a basic lateral flow assay in a sandwich format. Reprinted with permission from (Bahadır and Sezgintürk, 2016). C: Photo of a 2D μPAD. Reprinted with permission from (Hu et al., 2014). D: Photo of an electrochemical μPAD called NoSlip and its 3D-printed holder. Reprinted with permission from (Cunningham et al., 2016).

et al., 2018).

1.3. Limitations and challenges of developing PADs

A few reviews have compared different types of PADs (Hu et al., 2014; Mahato et al., 2017; Parolo and Merkoci, 2013; Syedmoradi et al., 2017). Here we summarize the performance of different PADs in Table 1 in terms of detection methods, advantages and limitations. Comparing with conventional quantitative techniques such as high-pressure liquid chromatography, gas chromatography mass spectrometry, and ELISA, which are proven to be sensitive and specific, PADs suffer from the relative low signal intensity and poor quantitative discrimination (Bahadır and Sezgintürk, 2016). Recently, many advances on PADs development have been investigated including signal amplification methods, multiplexed designs, improved quantification systems and the usage of new labels (Koczula and Gallotta, 2016). In this review we focus on summarising recent advances in signal amplification targeting to improve PADs sensitivity. We separate different signal amplification strategies applied on PADs (mainly LFAs and μPADs) in the following sections such as nanomaterial based, nucleic acid based, and engineering of PADs based signal amplification methods.

2. Nanomaterial based signal amplification methods

Nanomaterials can be used directly or as carriers of signal markers, and provide sensitive and selective detections. This section describes different nanomaterials such as gold nanoparticles (AuNPs), silver nanoparticles (AgNPs), magnetic nanoparticles (MNPs), quantum dots (QDs), upconversion nanoparticles (UCNPs), silica nanomaterials, carbon-based nanomaterials and some other nanomaterials, which are frequently used on PADs.

Table 1
Advantages and limitations of different types of PADs.

PADs	Detection methods	Advantages	Limitations
Dipstick assays	Optical (Parolo and Merkoci, 2013).	Rapid detection in minutes; Simple design; Ease of manufacturing and usage.	Optical detection only; Incapability to do quantitative analysis.
LFAs	Optical (Jauset-Rubio et al., 2016b); Fluorescent (Deng et al., 2018; You et al., 2017); Electrochemical (Koczula and Gallotta, 2016); Chemiluminescent (Park et al., 2015; Zangheri et al., 2015); Surface-enhanced Raman scattering (SERS) (Hwang et al., 2016; Lin and Stanciu, 2018; Sánchez-Purrà et al., 2017; Shi et al., 2018).	Ease of device preparation; Good stability with long shelf life; Quick detection (5–15 min); Simple and user-friendly operation; No sample pre-treatment required.	Limited sensitivity; Low efficiency of fluid flow due to matrix component i.e. obstruction of pores; Detection time influenced by viscosity of samples; Large sample volume (~100 μL); Semi-quantitative detections.
μPADs	Optical (Liu and Crooks, 2011); Fluorescent (Wu et al., 2014a); Electrochemical (Li et al. 2014a, 2014c); Electrochemiluminescent (Li et al. 2014a, 2014c; Liu et al., 2014c; Wu et al., 2015a); Chemiluminescent (Mahato et al., 2017); Photoelectrochemical (Ge et al., 2015; Wang et al., 2013b); SERS (Chen et al., 2016a).	No external instruments and complex fabrication processes required; Small sample volume (5–10 μL) for quick analysis (5–10 min); Compatibility with computers for real-time analysis; Capability for quantitative detections.	Difficulty in mass production; Lack of flow control; Limited accuracy; Possible complex and multiple steps; Long optimization time. Low volume handling requiring trained personnel.

2.1. AuNPs based signal amplification

AuNPs are the most commonly used nanomaterials in LFAs since they conjugate with other biomolecules easily to provide visible feedback due to the color change by aggregation and disaggregation (Rodriguez et al., 2016). The size of AuNPs is essential to the sensitivity of LFAs (Omidfar et al., 2010; Rodriguez et al., 2016), and 100 nm is believed to be the ideal size for LFA due to the high molar extinction coefficients, and the high reaction rate and signal per AuNP (Li et al., 2016; Zhan et al., 2017). AuNPs with the size larger than 100 nm provided poor quantitative performance in LFAs because of significant steric hindrance and strong light scattering (Li et al., 2016). AuNPs based signal amplification strategies are discussed in below sections including enlarging AuNPs conjugations, silver nucleation on AuNPs, modifying AuNPs with enzymes, catalytic metals or surface enhancement Raman tags.

2.1.1. Enlarging AuNPs aggregations

Enlarging AuNPs aggregations for a more intensive color on the test line is the straight forward method for signal amplification. Due to the rich amine groups, polyamidoamine was used for binding a large number of AuNPs-antibody conjugates to increase the sensitivity up to 50-fold for detection of bisphenol A (Peng et al., 2018). Moreover, Xu et al. used silica-based nanomaterials as the substrate to load AuNPs for designing a highly sensitive LFIA to detect proteins with a limit of detection (LOD) of 0.01 ng/mL (Xu et al., 2014). Thus, a large amount of AuNPs were loaded onto silica nanorods providing a purple color which was darker than that of AuNPs before forming aggregations. Another way of enlarging AuNPs aggregations for signal amplification is the dual-layered method (Chen et al., 2015; Wiriyachaiporn et al., 2014; Zhong et al., 2016) by conjugation of two different sizes of AuNPs. In particular, Chen et al. developed two types of dual AuNPs aided LFIAs for detection of *E.coli* O157:H7 (Chen et al., 2015). In the design, antibodies were used to link AuNPs to form anti-mouse-Ab-AuNPs structures in the sample and anti-*E.coli* O157:H7-mAb-AuNPs structures on the conjugation pad. Signal amplification was also realised in indirect LFIA method, in which anti-mouse-Ab-AuNPs composites were mixed with the anti-*E.coli* O157:H7-mAb-AuNPs composites in the sample before adding onto the sample pad. Different sizes of AuNPs (28 nm and 45 nm) bound together on the test line for sensitive detection with the help of additional linking agent (anti-mouse secondary antibody). The detection sensitivity was improved 100-fold in both types of LFIAs. Another dual-layered and double-targeted nanogold-based LFIA was designed to detect influenza A antigen with the sensitivity improved by a factor of 8 when compared with a conventional LFIA (Wiriyachaiporn et al., 2014). In this case, AuNPs in 15 nm and 40 nm were used on the LFIA. Although enlarging AuNPs aggregations is a relatively straight forward way of enhancing the signals, the reproducibility of forming the AuNPs aggregations will be a limitation. A strategy referred as “gold enhancement” is also able to enlarge AuNPs aggregation sizes using a reducing agent ($NH_2OH{\cdot}HCl$) (Ye and Xia, 2018) or loading gold enhancers (ultra-small 1.4 nm AuNPs) (Park et al., 2016b). The reducing agent based catalytic reaction can produce new AuNPs on the surface of initial AuNPs to enlarge the size of the aggregations and enhance the signals. For example, Bu et al. applied this strategy in a LFIA for detection of *Salmonella Enteritidis* (*S. Enteritidis*), and the signal was enhanced 100-fold due to the reaction between $HAuCl_4$ and $NH_2OH{\cdot}HCl$ (Bu et al., 2018).

2.1.2. Silver nucleation on AuNPs

Silver nucleation on gold is a well-investigated reaction and can be applied in biosensing area for signal amplification due to the simplicity and the achievable high sensitivity (Yu et al., 2015). The principle of silver enhancement on gold is that silver ions are reduced to silver on the surface of gold nanocrystals by the reducing agent surrounding vicinities of the silver grains. Thus the size of the nanocrystals will be expanded by the silver deposition (Liu et al., 2014b) to form a better contrast of black Ag-AuNPs on strips compared with that of original red AuNPs, which contributes to the enhanced signal (100-fold increase compared with AuNPs-based LFIAs) (Anfossi et al., 2013). Additionally, different silver salts have been used as the source of silver enhancement, such as silver lactate, silver nitrate and silver acetate (Kim et al., 2018b). Different from silver lactate and silver nitrate which are sensitive to lights, silver acetate is the best silver source for silver enhancement on gold without the need of controlling signal amplification reaction under dark conditions (Liu et al., 2014b). Rodríguez et al. found the sensitivity of prostate specific antigen (PSA) has been improved 3-fold with a LOD of ~0.1 ng/mL by dipping the LFIA strip into a silver nitrate and hydroquinone/citrate 1:1 buffer (Rodriguez et al., 2016). Furthermore, the silver enhancement strategy can also be applied by combining silver-reducing reagents with hybrid nanofibers for cardiac biomarker troponin I detection (Kim et al., 2018b). The silver-reducing reagents released from nanofibers deposited on AuNPs and darkened the color on the test line, and LOD was enhanced up to 10 times without affecting the assay time.

Nonetheless, the reduction reaction occurring on surface of AuNPs is easy to be activated even by the surrounding strip materials resulting in high background noise to affect the sensitivity. Thus, how to reduce the impact of materials on catalytic reactions should be considered when applying silver or gold enhancement methods. Meanwhile, silver and gold enhancement approaches require extra steps to add reagents (Chen et al., 2015). These limitations impede the wide application of silver and gold enhancement approach, and more efforts to realise one-step signal amplification are needed.

2.1.3. Modification of AuNPs with enzymes

AuNPs can be used as enzyme carriers to increase the enzyme catalytic abilities and induce LFA signal amplification (Koczula and Gallotta, 2016; Parolo et al., 2013). Due to the colorimetric property, horseradish peroxidase (HRP) can be conjugated to bioreceptors providing colourful signals as the output (Ye and Xia, 2018). Three different HRP based substrates (3,3′,5,5′-tetramethylbenzidine (TMB), 3-amino-9-ethylcarbazole, and 3,3′-diaminobenzidine tetrahydrochloride) were used in LFA strips, and TMB substrate provided the best limit of quantification (LOQ) (down to 200 pg/mL) due to the darker visible results (Parolo et al., 2013). Recently Panferov et al. used another enzyme alkaline phosphatase (ALP) to amplify the signal in detecting potato virus X with a LOD of 0.3 ng/mL (27 times lower than that of a conventional LFIA) (Panferov et al., 2017). Additionally, HRP can be combined with highly carbonized nanospheres (HCS) to enhance chemiluminescence signals of a PAD (Chen et al., 2018b). HRP functionalized HCS on a paper-based microfluidic CL chip was used for detection of carcinoembryonic antigen (CEA) with a LOD of 3 pg/mL (Chen et al., 2018b).

Using AuNPs loaded enzymes can achieve signal enhancement in a simple way, representing a potential method towards commercialisation. However, enzymes are relatively unstable, resulting in a shortened shelf life of assays and further reduce the detection accuracy. Moreover, the number of enzymes loaded is limited by the limited surface area of AuNPs (Ye and Xia, 2018). Strategies to address these challenges will be essential to the future wide applications.

2.1.4. Modification of AuNPs with catalytic metals

Well-controlled bimetallic nanoparticles can be used to enhance the signals as mimicking natural peroxidases when integrated into μPADs (Li et al., 2014b; Sun et al., 2014). Noble metal catalytic nanomaterials have been successfully used in LFIAs for signal amplification (Gao et al., 2017b; Loynachan et al., 2018) due to their high catalytic activity and stability even under harsh conditions (Loynachan et al., 2018). Considering the catalytic activity of platinum nanoparticles (PtNPs), Gao and his co-workers coated AuNPs with ultrathin Pt layers to form an integrated Au@Pt with LFIA (Gao et al., 2017b). Au@Pt obtained both

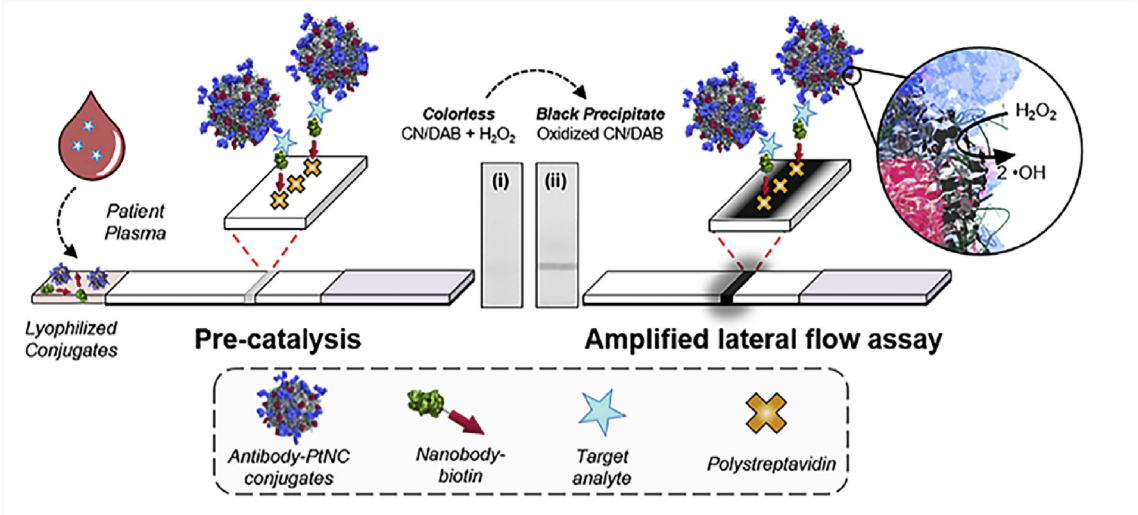

Fig. 3. The schematic design of the amplified LFIA using Pt nanocatalysts (PtNCs). Reprinted with permission from (Loynachan et al., 2018).

plasmonic activity from AuNPs and high peroxidase-like catalytic activity of PtNPs, and thus was able to generate a visible color change with the sensitivity enhanced by 2 orders of magnitude. While Loynachan et al. integrated an Au-Pt core-shell structure (PtNCs) into a LFIA to enhance the signal for detection of p24, a protein biomarker of HIV (Loynachan et al., 2018). AuNPs (15 nm) were used as seeds for Pt growth and the catalytic activity of PtNC increased the signal intensity by local deposition of dyes on the test line of LFIA with the sensitivity of femtomolar range (32.5 fM) (Fig. 3). Furthermore, Jiang et al. designed a sensitive LFIA strip to detect protein biomarkers p53 protein, by taking advantage of the peroxidase-like activity of Pt-Pd bimetal nanoparticles (NPs). (Jiang et al., 2016). The catalytic reaction between Pt-Pd NPs and TMB provides a highly stronger visible blue color comparing with that of AuNPs based LFAs, and the LOD was 0.05 ng/mL with a linear range of 0.1–10 ng/mL.

Bimetallic nanoparticles are also used for signal amplification on μPADs to detect CEA electrochemically (Ma et al., 2015; Sun et al., 2014). This strategy combined AuNPs modified paper working electrode (AuNPs-PWE) as sensor platform and Au-metal ions as tracing tags in one PAD to realise the dual signal amplification. Firstly, AuNPs-PWE accelerated the electron transfer rate in the paper sample zone to enhance the electrochemical signal due to its high conductivity and large surface area (Wang et al., 2015). Meanwhile, the Au-Ag bimetallic NPs as nanocarriers were used for loading numerous signal antibodies and produced an electrocatalytic response by reduction of H_2O_2 to further enhance the electrochemical signals with a LOD of 0.3 pg/mL (Sun et al., 2014). A Glucose oxidase (GOx) modified AuNPs were also used for dual signal amplification for developing a CL excited photoelectrochemical immunosensor to detect CEA at picomole level (Wang et al., 2015). Ge et al. used the bioconjugation of GOx functionalized nanoporous silver as signal tag and Au@Pt-PWE as sensor platform to enhance the sensitivity of a 3D origami immunodevice for detection of CEA and α-fetoprotein (AFP) with LODs of 0.3 pg/mL and 0.5 pg/mL, respectively (Ge et al., 2015). Additionally, Lan's group combined multibranched hybridization chain reaction with Pd-Au NPs to enhance the signal of photoelectrochemical immunoassay catalytically with the sensitivity of 0.33 pg/mL (Lan et al., 2016). Although catalytic metals modified on AuNPs are helpful to increase sensitivity of PADs, the poor reproducibility and stability of these conjugated AuNPs are expected to limit the commercialisation of these type of PADs.

2.1.5. Modification of AuNPs with surface-enhanced Raman scattering (SERS) tags

SERS technique adopting AuNPs based SERS tags, with ultrasensitive and multiplexed detection capability, has also been applied on aptamer and antibody-based PADs for signal enhancement (Fu et al., 2016; Wang et al., 2017; Xiao et al., 2018; Zeng et al., 2018). In a SERS-based LFA kit, AuNPs-based SERS tags were used as detection probes due to their high SERS enhancement effect (Wang et al., 2017). By monitoring characteristic SERS signals of the Raman reporter labelled AuNPs on the test line, highly quantitative analysis of the target can be achieved (Park et al., 2016a). In particular, Fu et al. developed a SERS-based LFA for HIV-1 DNA detection with a LOD of 0.24 pg/mL, which was at least 1000 times more sensitive comparing with other colorimetric or fluorescent detection methods (Fu et al., 2016). Also, Wang and the group labelled SERS nano tags with detection DNA probes for multiplexed and simultaneous determination of dual DNA markers (associated with Kaposi's sarcoma-associated herpesvirus (KSHV) and bacillary angiomatosis (BA)) with high sensitivity (Wang et al., 2017). The LOD of the designed LFA strip for KSHV (0.043 pM) and BA (0.074 pM) were around 10,000 times more sensitive than that of PADs using the aggregation-based colorimetric method. Several reports about SERS application on μPADs (Chen et al., 2016a) or on antibody-based PADs for sensitive detection of a spectrum of analytes, for instance, proteins (Rong et al., 2018), hormone (Choi et al., 2017b), cardiac biomarkers (Zhang et al., 2018), microorganisms, metabolism products (Hwang et al., 2016; Park et al., 2016a; Wang et al., 2018) and chemical compound (bisphenol A) (Lin and Stanciu, 2018) have been addressed. LFIA in combination with Au based SERS probes exhibited superior performance in terms of sensitivity of neuron-specific enolase in blood plasma-containing sample matrix with a LOD of 0.86 ng/mL (Gao et al., 2017a). SERS-based PADs are more sensitive than conventional LFAs, however, the reproducibility is still a major obstacle for real sample detection. In addition, the complexity of making AuNPs modified with SERS tag, and the availability of hand-held SERS detectors are factors limiting the wide applications of this signal application on PADs.

Despite of the excellent properties of AuNPs, there are still drawbacks of using AuNPs for signal amplification on PADs, such as relative high cost, unsteadiness (Deng et al., 2018) and the inherent plasmonics (Gao et al., 2017b). Apart from AuNPs, other nanomaterials have also been investigated and used for signal enhancement, which will be discussed in below sections.

2.2. Silver nanoparticles (AgNPs) based signal amplification

The high molar extinction coefficient of AgNPs improves the visibility based on the difference in optical brightness, and thus increases

the sensitivity of UV–visible spectroscopic detection (Ratnarathorn et al., 2012). AgNPs are often used together with AuNPs for signal amplification, such as the silver nucleation on gold (discussed in Section 2.1.2) and as silver layer on 3D μPADs (Li et al., 2014d). In particular, a cuboid silver (CS) layer with high conductivity was grown on the surface of cellulose fibers from AgNPs seeds in the paper sample zone for simultaneous electrochemical detection of cancer antigen 125 (CA125) and carcinoma antigen 199 with LOD of 0.02 and 0.04 mU/mL, respectively.

AgNPs are more affordable than AuNPs (Malekzad et al., 2017) and as noble metal nanoparticles, they are visible without external excitation source or emission sensor (Yen et al., 2015). Comparing with other nanomaterials, AgNPs have similar limitations as noble metal nanoparticles such as inherent plasmonics, relatively poor stability and toxicity.

2.3. Magnetic nanoparticles (MNPs) based signal amplification

Besides offering fast separation capability in magnetic field, MNPs or magnetic beads are brown (Oliveira-Rodriguez et al., 2017) and provide low background noise, which make them ideal probe materials on PADs (Huang et al., 2016b). Strategies of using MNPs for signal enhancement have been widely used in electrochemical biosensing (Hasanzadeh et al., 2015). Compared with the conventional LFIAs, sensitivity of detecting furazolidone metabolite of 3-amino-2-oxazolinon was improved to at least 10-fold using MNP labelled antibodies in a dual-probe network complex with a LOD of 0.044 ng/mL (Yan et al., 2018). Similarly, Liu et al. linked the secondary MNPs with the detection MNPs through bio-streptavidin interaction for signal improvement in LFIA for CEA detection with a LOD of 0.25 ng/mL (Liu et al., 2016a). MNPs are generally used with AuNPs (Razo et al., 2018; Ren et al., 2016; Xia et al., 2016a) for signal enhancement in LFIAs. For example, MNPs and AuNPs were conjugated through biotin-streptavidin reaction and applied a LFIA for detection of potato virus X with a LOD of 8 ng/mL (32 times more sensitive than the non-enhanced LFIA) (Razo et al., 2018). Xia's group used MNPs together with AuNPs to form gold magnetic bifunctional nanobeads on an immunochromatographic test for sensitive detection of *Salmonella choleraesuis* with a sensitivity of 5×10^5 CFU/mL (Xia et al., 2016a). MNPs were also able to pre-concentrate the AgNPs on detection electrode of PADs for sensitive detection of proteins, nucleic acids and microbes (Scida et al., 2014).

MNPs are often used for amplifying signals on PADs because they are magnetically controllable and can provide low background noise with their dark color. However, similar as other nanomaterials, MNPs have limitations such as the relative high cost and the aggregation issue. Thus proper surface coating of MNPs to minimize aggregation is needed before the wide applications. (Jiang et al., 2016; Mohammed et al., 2017).

2.4. Quantum dots (QDs) based signal amplification

QDs are widely used as fluorescent labels (Shao et al., 2018; Shen et al., 2017; Xiao et al., 2017) on PADs due to their unique optical properties such as excellent signal brightness, size-tuneable light emission, strong stability against photobleaching, and low background signal. Sapountzi et al. designed a dipstick-type PAD for visual detection of nucleic acids under a UV lamp using QDs as signal reporters (Sapountzi et al., 2015), and the LOD was down to femtomole. Taranova et al. used three types of QDs with different emission peaks (red, yellow and green) in an immunochromatographic assay (ICA) for sensitive and simultaneous detection of antibiotics in milk with the LOD 80–200 times lower than those provided by ELISA (Taranova et al., 2015). In order to solve the chemical and colloidal instability in physiological environment with the pure QDs, strategies of encapsulating or doping QDs in polymers or other carriers have been widely investigated for signal amplification on PADs (Ouyang et al., 2017). Quantum dot nanobeads (QBs) are polymer nanobeads doped with numerous QDs possessing a substantially higher fluorescent intensity than QDs (Shao et al., 2018). QBs have been used for signal amplification on PADs (Duan et al., 2017; Hu et al., 2017; Li et al., 2014e; Ren et al., 2014; Shao et al., 2018; Shen et al., 2017; Xiao et al., 2017). Li et al. prepared QBs by encapsulating QDs within modified poly (*tert*-butyl acrylate-*co*-ethyl acrylate-*co*-methacrylic acid) which were used as signal-enhancement agent on an ICA to detect PSA (Li et al., 2014e). Comparing with ICA which used QDs encapsulated by commercial 11-mercaptoundecanoic acid, the QBs based ICA was more stable and sensitive (the LOD was enhanced by approximately 12-fold). Also, Ren et al. synthesized highly luminescent QBs by encapsulating CdSe/ZnS for signal amplification on ICA for aflatoxin B_1 detection, and the sensitivity was 2 orders better than that of the AuNPs-based ICA (Ren et al., 2014). While Hu et al. used fluorescent nanosphere containing CdSe/ZnS QDs for signal enhancement to detect C-reaction protein. The assay was 257-fold more sensitive than a conventional AuNPs-based LFA (Hu et al., 2016).

In order to further improve the assay sensitivity Deng's group applied the target-recycled nonenzymatic amplification strategy onto the QDs-labelled aptamer-based PAD for rapid and sensitive detection of miRNA (Deng et al., 2017). In the system, dual signal amplification was realised by using QDs as signal labels together with the target-recycled nonenzymatic amplification strategy (will be explained in Section 3.1.3) based on sequence-specific hairpins strand displacement process to improve the sensitivity. Thus, the detection sensitivity ranged from 2 fM to 200 fM with a limit of 200 aM by using only 20 μL of sample, and it was 10-fold more sensitive than that of a conventional AuNPs-based test strip. Although QDs based signal amplification on PADs was very efficient, QDs are detrimental to health and the environment, which still needs to be addressed before their wide application in POC diagnostics (Zhang et al., 2017).

2.5. Lanthanide nanoparticles based signal amplification

Upconversion nanoparticles (UCNPs), as a type of lanthanide nanoparticles, can be excited by near infrared (NIR) light and emit visible lights, are emerging as fluorescent labels for bio-detections of proteins, small molecules, and oligonucleotides (He et al., 2016). In comparison with the traditional fluorescent labels such as QDs, UCNPs possess outstanding properties such as low-auto fluorescence, photostability, narrow emission spectrum and less toxic elements with multicolour tuneable property (Jin et al., 2017). UCNP based PADs have attracted attention recently with broad applications in biomedicine area for detection of biomarkers with improved performance (Liang et al., 2017; You et al., 2017; Zhao et al., 2016). A new strategy called luminescence resonance energy transfer (LRET) (FRET is termed as LRET when rare earth materials are used (Wang et al., 2009)) can enhance the sensitivity in biosensing, especially when combining UCNPs with AuNPs in the assay for drug detections on PADs (Chen et al., 2018a). The PAD was able to qualitatively analyse cocaine detection by naked eyes based on luminescence signals (He et al., 2016). With the aid of the smartphone camera, the LOD of cocaine was down to 10 nM in aqueous solution and 50 nM in human saliva (He et al., 2016). Based on LRET, Chen et al. developed a PAD using UCNPs combined with gold nanorods (AuNRs) for sensitive detection of exosomes with a LOD of 1.1×10^3 exosome particles/μL (Fig. 4) (Chen et al., 2018a). In this design, DNA aptamers specific to CD63 protein were split into two different sequences called capture probe (CP) and detection probe (DP). Before immobilizing onto the sodium periodate oxidized filter paper, UCNPs and CP were first modified by polyethylenimine and an amino due to the reaction between the amino and the aldehyde group of paper. CP was modified by AuNPs. With the presence of exosomes, CD63 protein on the surface of exosomes has the affinity of both CP and DP bring both of CP and DP around exosomes which significantly reduced the distance between UCNPs and AuNRs to allow the LRET to take place. Then the

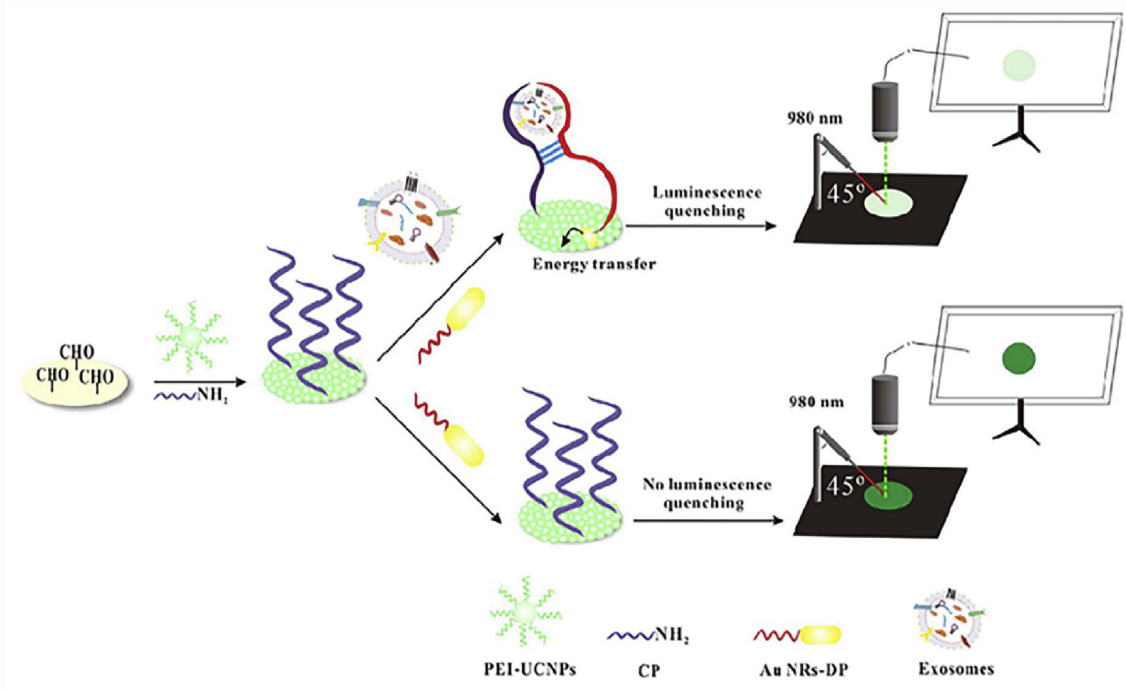

Fig. 4. The mechanism of the paper-based aptasensor for detection of exosomes. Reprinted with permission from (Chen et al., 2018a).

green luminescence quenching occurred under 980 nm excitation. In contrast, when there was no exosome in the sample, CP and DP would not combine together and no LRET occurred.

Other lanthanide nanoparticles such as europium nanospheres were also used on PADs as immunoreagents when conjugating to antibodies (Li et al., 2018; Wang et al., 2016a) for signal enhancement. UCNPs and other lanthanide nanoparticles provide a sensitive, multiplexed, and quantitative way of detection, however, high costs, complicated preparation procedures together with difficulties of interpretation by the naked eye in natural light conditions make their applications limited (Zhang et al., 2017). Especially, quantifying the lanthanide nanoparticles based PADs requires special laser detector which limits POC applications.

2.6. Silica nanoparticles based signal amplification

Silica nanoparticles, as a type of semi-conductive material, are often used together with QDs for signal amplification on PADs (Liu et al., 2014c; Qiu et al., 2017; Wu et al., 2014a; Zhao et al., 2017), not only due to their good water dispersibility, surface functionality and biocompatibility, but more importantly, silica nanoparticles can enhance the chemical stability and reduce the toxicity of QDs by excluding the diffusion of heavy metal ions from the environment (Zhao et al., 2017). Specifically, CdTe QDs embedded silica nanoparticles, on which detection antibodies were labelled, were used as signal enhancement label in a paper-based immunodevice for fluorescent detection of AFP with a LOD of 0.4 pg/mL. The detection sensitivity was improved 4.7-fold comparing with the antibody-QD conjugation (Zhao et al., 2017). Another example using silica nanoparticles with QDs for signal enhancement was reported by Liang et al., (2016). Signals were amplified using conjugations of mesoporous silica nanoparticles and QDs labelled with detection antibodies. The proposed μPAD was used for detection of cancer cells with the LOD of 62, 70, and 65 cells/mL for MCF-7, HL-60, and K562 cells, respectively. This study demonstrated the potentials of mesoporous silica nanoparticles on PADs due to their various outstanding properties, such as uniform pore diameters, large surface-to-volume ratio, and capacity in surface functionalization (Liang et al., 2016).

2.7. Carbon nanomaterials based signal amplification

Carbon-based nanomaterials including carbon nanotubes and graphene are also used for signal enhancement on PADs. Recently, taking advantages of the excellent properties of carbon nanotubes, such as high specific surface area and high signal-to-noise ratio (Huang et al., 2016b), Qiu's group described an aptamer-based LFA for DNA detection using carbon nanotube as signal tag (Qiu et al., 2015). The LOD was 12.5 times lower than that obtained by AuNPs-based LFAs. Additionally, Yao's group developed an aptamer-based LFA for detection of mercury ions using multi-walled carbon nanotubes as labelling substrate to improve the strip stability and sensitivity, and the sensitivity improved 10-fold when comparing with the conventional AuNPs based PADs (Yao et al., 2016). Amorphous carbon nanoparticles (ACNPs) being different from the well-developed carbon nanotubes were reported to be more sensitive than AuNPs on PADs by providing a strong dark color. The outstanding advantages of ACNPs include high stability, low toxicity, ease of conjugation and preparation, and no need for activation (Zhang et al., 2017). A multiplexed ACNP-LFA was developed for detecting three *Fusarium* mycotoxins with the LOD improved 8-fold comparing with AuNPs-LFAs and 2-fold comparing with QD-LFAs in buffer (Zhang et al., 2017).

Graphene is a 2D carbon nanomaterial with high conductivity and high specific surface area (Wang et al., 2016b), and also amenable to microfabrication techniques (Yang et al., 2010)., which makes graphene a good signal tag in electrochemical PADs for POC usage. Wu et al. developed an electrochemical μPAD for multiplexed detection of four different cancer biomarkers by modification of μPAD with graphene and silica nanoparticles to amplify the signal (Wu et al., 2013). The electron transfer was accelerated by using graphene on the surface of the immunodevice, and as for the silica nanoparticles labelled with the signal antibodies, a large amount of HRP could be introduced onto silica nanoparticle carriers to maximize the ratio of enzyme per assay. In this way, the signal was enhanced with a LOD down to sub pg/mL level (Wu et al., 2013). Moreover, decorating graphene with other metallic nanoparticles such as AuNPs were also studied on PADs for enhance the sensitivity. Wang's group fabricated a μPAD for sensitive electrochemical detection of CEA using amino functionalized

graphene/thionine/AuNPs nanocomposites for signal amplification with a LOD of 10 pg/mL (Wang et al., 2016b). An electrochemical device based on reduced graphene oxides/platinum nanocomposites in a shape of nanocauliflower was used for detection of small molecules (glucose) or pathogenic bacteria (*Escherichia coli* O157:H7). The LODs for glucose and *E. coli* O157:H7 were 0.008 ± 0.02 μM and 4 CFU/mL, respectively (Burrs et al., 2016). Moreover, a paper-based LFIA based on the photoluminescence quenching ability of graphene oxide and the excellent photophysical properties of quantum dots nanocrystals was investigated for detection of pathogen (*E. coli*) with LODs of 10 CFU/mL in standard buffer and 100 CFU/mL in bottled water and milk (Morales-Narvaez et al., 2015). Carbon based nanomaterials are increasingly attractive on PADs due to the low cost and unique properties described above. However, the sensitivity needs to be further increased by combining with other nanomaterials.

2.8. Other nanomaterials based signal amplification

Apart from the above-mentioned nanomaterials, some other nanomaterials were also applied on PADs to provide sensitive results. For instance, liposomes are used for signal enhancement as a large number of signal molecules can be released by disrupting small amounts of liposomes (Chapman et al., 2015; Leem et al., 2014). Chapman et al. used liposomes as enzyme substrate and multivalent nanoparticle networks to amplify the signal of $hPLA_2$ detection (Chapman et al., 2015). The LFA included two signal amplification mechanisms (signal enhancement by releasing multiple PEG linkers from a signal liposome disruption and the network of AuNPs forming on the test line by multivalent interactions). The LODs of $hPLA_2$ was 1 nM in serum and 0.1 nM in buffer, This PAD provided an accurate and sensitive diagnosis of $hPLA_2$ in acute pancreatitis clinically (Chapman et al., 2015). Limitations of using liposomes on PADs include their instability and the difficulties in flow control. Furthermore, long synthesis procedures together with challenges in controlling the size of liposomes affect the reproducibility of liposome based PAD in real applications (Quesada-Gonzalez and Merkoci, 2015).

Polymerization-based amplification (PBA) is a novel amplification strategy which is applicable on PADs. Badu-Tawiah et al. used the PBA method for sensitive visual protein detection in paper-based immunoassays (Badu-Tawiah et al., 2015). In this work, photoinitiator molecules initiate a free-radical polymerization reaction and generate an interfacial hydrogel in the presence of light. A pH indicator was used to detect the formation of hydrogel on the assay providing rapid and quantitative results with the sensitivity of 7.2 nM (0.56 μg/mL) for detect ion of *Plasmodium falciparum* histidine-rich protein 2. Long chain polymeric materials with rich surface chemistry can be modified with molecules to provide extra signal tags like nanoparticles (Wu et al., 2014b). Wu et al. designed a paper-based microfluidic electrochemical immunodevice for multiplexed detection of cancer biomarkers by applying a polymerization-assisted signal amplification method (Fig. 5). Growth of the long chain polymeric materials provides multiple sites for HRP coupling further amplifying the electrochemical signal. The device was able to detect four cancer biomarkers (CEA, AFP, CA125 and carbohydrate antigen 153 (CA153)) with LODs of 0.01, 0.01, 0.05 and 0.05 ng/mL, respectively. Additionally, semiconducting polymer dots (Pdots) have been used as a new type of biocompatible fluorescent probe due to their excellent brightness. Pdot-based fluorometric LFIA was developed for multiplexed and quantitative screening of tumor markers (PSA, AFP, and CEA), and the LOD was at least 2 orders of magnitude lower than that of conventional fluorometric LFIAs (Fang et al., 2018).

Apart from QDs and UCNPs described in Section 2.4 and 2.5, other fluorescent nanomaterials such as the organic molecules have also been applied on PADs for sensitive detections. For example, the near infrared dyes can be conjugated to antibodies to form the detection complex in LFIA for detection of four antibiotic residue families in milk which were β-lactams, tetracyclines, quinolones and sulphonamides with qualitative LOD of 8 ng/mL, 2 ng/mL, 4 ng/mL and 8 ng/mL respectively (Chen et al., 2016b).

Although nanomaterials possess excellent properties for signal amplification on PADs, such as large surface area, biocompatibility, size-tuneable light emission and et al., wide applications of using these nanoparticles for signal amplification will be hurdled significantly due to their chemical instability, low reproducibility, the complexity of applying them on PADs, and the requirement of time-consuming detection process or advanced laboratory equipment for some types of nanoparticle based PADs (Jiang et al., 2016; Xu et al., 2014). The pros and cons of using different nanomaterials on PADs are summarised in Table 2.

3. Nucleic acid based signal amplification methods

PADs using aptamers as recognition molecules have recently attracted wide attention because aptamers have significant advantages over antibodies in terms of superior stability, low cost and less batch-to-batch variation (Li et al., 2015). Additionally, the feasibility of applying nucleic acid based signal amplification on PADs is another most important advantage of aptamer to be used on PADs, which favours the detection of trace analytes (especially DNAs and RNAs) using PADs (Cao et al., 2018). Nucleic acid based signal amplification strategies applied for PADs can be achieved through nucleic acid synthesis, and the recent CRISPR/Cas biosensing system although few studies report their applications on PADs.

3.1. Signal amplification through nucleic acid synthesis

Nucleic acid amplification is a promising area for developing sensitive paper-based POC diagnostics and it is often used for virus or infection detection to amplify the amount of nucleic acid. To amplify the amount of nucleic acid, different methods of nucleic acid synthesis have been developed accordingly. PCR is a best known and extensively used technique which has been used for nucleic acid amplification in research laboratories and hospitals. Nonetheless, this technology needs thermal cycling due to the need of accurate temperature control (Tian et al., 2018), also, PCR is currently not applicable on PADs for detection (Magro et al., 2017). Hence, isothermal nucleic acid amplification techniques, such as rolling circle amplification (RCA) (Feng et al., 2017; Hui et al., 2018; Kim et al., 2018a; Liu et al., 2016b; Wu et al., 2015b), loop-mediated isothermal amplification (LAMP) (Choi et al. 2016a, 2016b; Connelly et al., 2015; Rodriguez et al., 2015; Roskos et al., 2013; Seok et al., 2017; Xu et al., 2016), strand-displacement amplification (SDA) (Chen et al., 2014; Deng et al., 2018; Huang et al., 2016a; Phillips et al., 2018), recombinase polymerase amplification (RPA) (Chao et al., 2015; Cordray and Richards-Kortum, 2015; Crannell et al., 2016; Jaroenram and Owens, 2014; Jauset-Rubio et al. 2016a, 2016b), helicase dependent amplification (HDA) (Shetty et al., 2016), nucleic acid sequence-based amplification (NASBA) (Luo et al., 2014) and so on, are used to amplify the signal reported by PADs (Phillips et al., 2018) offering on-site detection of various targets with high sensitivity and specificity. Since there are many reviews reporting nucleic acid testing for PADs (Craw and Balachandran, 2012; Tian et al., 2018) and isothermal nucleic acid amplification mechanisms (Ali et al., 2014; Li and Macdonald, 2015), this review will not detail these nucleic acid amplification methods. Instead, we discuss the pros and cons of popular nucleic acid amplification methods such as, RCA, LAMP, and RPA when they are used on PADs (Table 3).

RCA, as a versatile isothermal amplification technique, has been applied on PADs for signal amplification since the process is able to produce spatially condensed micron-sized ssDNAs which are detectable as signal amplified molecules (Kim et al., 2018a). RCA products can be directly labelled with fluorescent dyes or nanoparticles such as AuNPs, MNPs, QDs for fluorescent, colorimetric or electrochemical detection

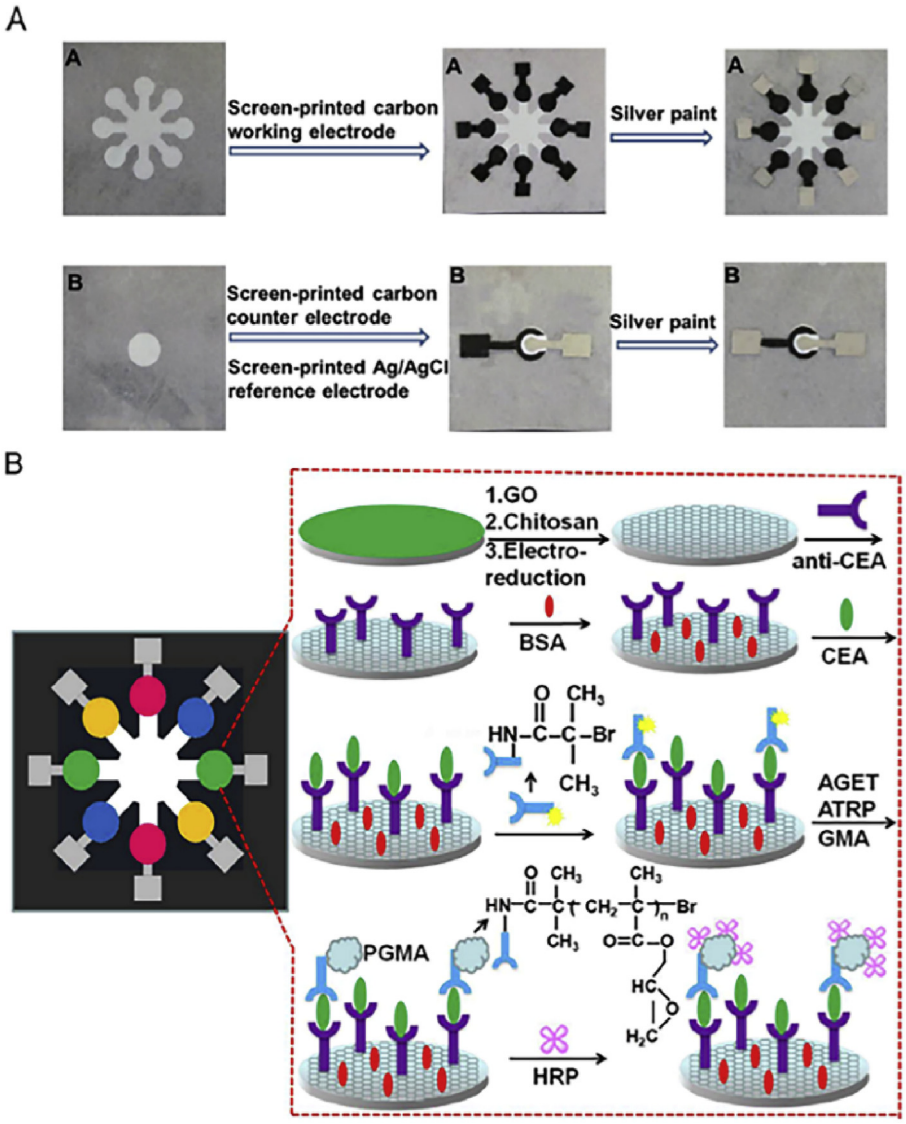

Fig. 5. (A) Fabrication process of the μPAD. (B) The scheme illustrates the mechanism of the device. Reprinted with permission from (Wu et al., 2014b).

(Ali et al., 2014). Kim et al. developed a novel radial flow assay using RCA combined with AuNPs probes to amplify signals for the colorimetric detection of Hg^{2+} with LOD of 22.4 nM (Kim et al., 2018a) (Fig. 6I). RCA can also be integrated into the device in a solid phase. Liu et al. observed that RCA reactions could be performed on a patterned paper substrate printed with DNA primers providing enhanced detection kinetics (around double) comparing with that performed in solution due to the enhanced localization of the reagents (Liu et al., 2016b). Recently by applying the aptamer-assisted isothermal amplification, Hui's group developed a novel RNA aptamer-based PAD for detection of adenosine triphosphate and an aptamer-based PAD for detection of glutamate dehydrogenase with outstanding sensitivity and selectivity (Hui et al., 2018). In this design, the physically detachable paper-based biosensor consisted two reaction zones and a bridge between them. The aptamer was released as soon as the bridge connected the two zones, and the RCA process was then triggered providing a colorimetric signal output. To be differently, applying RCA in immunoassays, Wu et al. developed a novel ECL paper-based origami device for detection of IgG antigen with a LOD down to 0.15 fM and a linear range of 1.0 fM-25 pM (Wu et al., 2015b). In the device, a cascade signal amplification strategy was applied, which combined the RCA technique with oligonucleotide (probe) functionalized carbon dots.

In order to integrate LAMP into PADs, Connelly and his group reported a PAD called “paper machine” which used LAMP method for nucleic acid amplification to detect *E.coli* with a LOD of 5 cells (Connelly et al., 2015). The device combined steps (sample introduction, wash with buffers, and LAMP amplification) with detection in a disposable, compact sliding-stripe, and the signal readout was achieved by a portable UV source or a smartphone. The “paper machine” replaced many benchtop instruments needed for nucleic acid amplification, such as the centrifuges, pipettes and vortex mixers, while it still needed the extra instrument for analysing the result and an incubator to heat the device (Connelly et al., 2015). To solve this problem, Choi et al. created a handheld battery-powered device to replace the incubator, and integrated LAMP and LFA together to achieve a portable, cost-effective PAD with a LOD of as low as 3×10^3 DNA copies (Choi et al., 2016a). Moreover, Xu et al. designed a multiplexed origami PAD for visible detection of *Plasmodium* DNA in whole blood using LAMP with a LOD down to 5 parasites/μL (Xu et al., 2016), and LAMP integrated LFIA was also applied for detection of bacteria (*P. aeruginosa* and its toxin genes) with a LOD of 20 CFU/mL (Chen et al., 2016c).

SDA can also be realised based on the reaction between hairpin DNA probes (also called padlock probes) and exonucleases, nicking endonucleases (NEase) or polymerases (Liu et al., 2013). However, nicking endonuclease is sequence-dependent while polymerase is primer-dependent (Chen et al., 2014). Thus, exonuclease III (Exo III) is

Table 2
A brief summary of using different nanomaterials for signal amplification applied on PADs.

Nanomaterial used	Popular signal read-out methods on PADs	Advantages	Limitations
AuNPs	Colorimetric; Electrochemical; SERS.	Rich surface chemistry; Optical visibility.	Relative high cost; Poor stability; Limited sensitivity.
AgNPs	Colorimetric; Electrochemical.	Optical visibility; Capability to enhance sensitivity used with AuNPs.	Toxicity; Poor stability.
MNPs	Colorimetric; Electrochemical.	Low background noise involved; Good biocompatibility; Magnetically controllable process.	Relative high cost; Proper surface coating required.
QDs	Fluorescent.	Excellent signal brightness and low background signal; Size-tunable light emission; Photostability; Broad ultraviolet absorption and narrow fluorescent emission spectra.	Poor stability in physiological environment; Toxicity to health and the environment.
Lanthanide nanoparticles	Fluorescent.	Low-auto fluorescence; Photostability; Narrow emission spectrum; Less toxic elements multicolour tuneable property.	High cost; Complicated preparation steps; Requirement of special light conditions which limits the POC applications.
Silica nanoparticles	Fluorescent.	Good water dispersibility; Rich surface chemistry for binding biomolecules; Good chemical stability; Less toxicity than QDs.	Limited sensitivity (need to be used together with QDs for sensitive detections).
Carbon nanomaterials	Colorimetric; Electrochemical.	High signal-to-noise ratio; Low toxicity; Simple preparation steps; Low cost.	Limited sensitivity.
Liposomes	Colorimetric.	Excellent encapsulation efficiency; Ability to encapsulate a wide range of different signalling molecules;	Poor stability; Complicated preparation steps.

used for developing a more universal detection platform due to the sequence-independent property and often involves in the target recycling strategy (Huang et al., 2016a). An Rxo III-aided target recycling strategy was used for sensitive DNA detection (Fig. 6.II). On the strip, the toehold-medicate strand displacement reaction together with the Exo III-assisted signal amplification provided the amplified detection of Hg^{2+}. The Exo III enzyme catalyzed the removal of blunt 3′ end of the opened hairpin DNA and released Hg^{2+} from the T- Hg^{2+} -T base pairs (process b in Fig. 6.II (A)). However, Exo III did not remove the protruding 3' terminus of the assistant DNA, and thus the assistant DNA and Hg^{2+} could be recycled and started a new cycle of reactions including toehold binding, branch migration, displacement reaction, and strand digestion. This mechanism allowed a small amount of Hg^{2+} to trigger the digestion of a large amount of hairpin DNA into single-stranded DNAs which were then applied onto the sample pad for visual detection. The LOD for Hg^{2+} (1 pM by naked eyes) by using the Exo III-aided signal amplification strategy was 2 orders of magnitude better than that using the LFA without signal amplification (Chen et al., 2014).

HDA and NASBA were applied on PADs although they are no popular. All HDA reagents except the DNA template can be dried and stored on paper substrates. HDA technique was used for amplifying a fragment of *Mycobacterium tuberculosis* DNA in the viscous artificial sputum on a BSA treated paper substrate using cheap heat sources, such as hand warmers or hot plates providing 65 °C environment for HDA reaction (Shetty et al., 2016). The assay can detect as little as 100 copies (in ~5 μL) of the template on the paper substrate in 10 min with the help of a fluorescent dye. Luo et al. applied a NASBA technique in tubes for amplifying the hlyA mRNA, an RNA marker in *Listeria monocytogenes* (Luo et al., 2014), and the amplification products were then applied to LFA strips which used AuNPs sandwich format for colorimetric detection with a LOD of 0.5 μg/μL genomic RNA within 15 min. NASBA shows potential in POC diagnostics, however, there are many limitations of applying the amplification process on paper matrix due to the requirement of the denaturation step. Moreover, NASBA only amplifies RNA targets, thus, this further limits its wide usage for POC diagnostics on PADs (Choi et al., 2017a; Shetty et al., 2016).

Various isothermal nucleic acid techniques provide minimal equipment settings without external thermocycler, and can be used for cost-effective, sensitive POC diagnostics on PADs with different advantages (Table 3). RCA, LAMP, and SDA utilize the strand displacement activity of polymerase to displace strand from dsDNA. But RPA, HDA and NASBA use additional enzymes such as recombinase, helicase and RNaseH to separate dsDNA or DNA-RNA hybrid into signal stranded forms for further amplification (Reid et al., 2018). Along with their advantages, there are also challenges regarding the nucleic acid amplification strategies on PADs. Currently, most of the isothermal nucleic acid amplification reactions are performed in tubes or cartridges before dropping the products on to PADs for detection (Luo et al., 2014; Phillips et al., 2018) since there are limitations of integrating whole nucleic acid amplification reaction onto paper-based substrates such as the temperature control and stability of the enzymes in solid phase. Especially, RPA was performed using the commercial kit such as TwistAmp Basic Kit (KwistDx, UK) ((Kersting et al., 2014; Zhao et al., 2019)), and the LFA strips were then dipped into the RPA products for sensitive colorimetric DNA/RNA detection by binding to tag-specific antibodies labelled with nanoparticles on the test strip (Ghosh et al., 2018; Hu et al., 2019; Jaroenram and Owens, 2014; Jauset-Rubio et al., 2016a; Li et al., 2019a; Liu et al., 2019; Zhao et al., 2019). Moreover, isothermal nucleic acid amplifications are inhibited to some extent when all of the reagents were absorbed into the membrane without excess liquid (Linnes et al., 2016). Thus, the selected membrane is crucial for the applications on PADs. Although the optimal design for membranes is still undiscovered, Linnes et al. reported that polyethersulfone was able to provide an optimal support for paper-based NAT as a new membrane material tested in both LAMP and HDA (Linnes et al., 2016). Also, challenges such as purification, massive production and storage of the products exist in this field. With the help of computer-aided methods (e.g. web-based software), the primer sequences and DNA nanostructures become predicable and designable, which will eliminate the undesired interactions and further improve the

Table 3
A summary of advantages and challenges for different isothermal nucleic acid amplification techniques used on PADs.

Amplification techniques	Advantages	Challenges
RCA	Simple reaction mechanism; Low reaction temperature: 37 °C (Ali et al., 2014); Versatile technique with designable circular templates (Ali et al., 2014); Compatibility with the device in a solid phase (Liu et al., 2016b).	Low tolerance to unprocessed biological samples (Shetty et al., 2016); Highly purified templates required (Ali et al., 2014); Instability of long products which tends to aggregate (Ali et al., 2014).
LAMP	High sensitivity and specificity (Notomi et al., 2000); The availability of commercial kits reduces the assay complexity (Craw and Balachandran, 2012); No requirement for additional enzymes (Reid et al., 2018); Robust reaction; Capability to amplify RNA using RT-LAMP for (Kaarj et al., 2018; Rodriguez et al., 2015).	Requirement of carful design in Primer sets (Jauset-Rubio et al., 2016b); Relative high reaction temperature:60–65 °C (Magro et al., 2017); Risk of contamination; 95 °C post-LAMP denaturation step prior to detection required (Jauset-Rubio et al., 2016b); Limited multiplexity (Jauset-Rubio et al., 2016b).
SDA	Low reaction temperature: 37 °C (Li and Macdonald, 2015); Simple design; Capability to amplify short oligonucleotides (50–120 base pairs) (Li and Macdonald, 2015).	Pre-heating step to denature dsDNA required (Craw and Balachandran, 2012); Low sensitivity to DNA background and the co-amplified product will influence the efficiency (Craw and Balachandran, 2012; Li and Macdonald, 2015); Restriction endonuclease and DNA polymerase required after denaturing (Craw and Balachandran, 2012). Low efficiency (compared with LAMP) (Li and Macdonald, 2015);
RPA	Simplified assay setup (Li et al., 2019a); Low reaction temperature: 37–42 °C (Li and Macdonald, 2015); Quick reaction time (< 20 min) (Rivas et al., 2018); High sensitivity compared with conventional PCR (Li et al., 2019a); Conventional operation (commercial kit available) (Li et al., 2019a).	Inhibition in whole blood (Rohrman and Richards-Kortum, 2015); Consecutive rehydration and addition of magnesium acetate required for commercial kit (Shetty et al., 2016).
HDA	Only one set of primers required (Shetty et al., 2016); Capability to amplify DNA from crude samples such as blood (Shetty et al., 2016) and cells (Linnes et al., 2015); Single incubation temperature (Shetty et al., 2016); One-off reaction components without further user intervention (Shetty et al., 2016).	Moderate sensitivity (Choi et al., 2017a); Relatively high reaction temperature: 60–65 °C.
NASBA	Less contamination (Li and Macdonald, 2015); Capability to amplify RNA even in the presence of genomic DNA (Li and Macdonald, 2015); 65 °C annealing temperature for primer 1 and 41 °C for the rest of the reaction (Li and Macdonald, 2015); Capability to amplify short oligonucleotides (120–250 base pairs) (Li and Macdonald, 2015);	95 °C denaturation step required (Li and Macdonald, 2015); Enzymes required after the annealing step (Li and Macdonald, 2015); Limited usage for POC diagnostics, only amplifies RNA targets (Choi et al., 2017a; Shetty et al., 2016).

performances (Craw and Balachandran, 2012; Zhao et al., 2008).

3.2. CRISPR/Cas systems used for signal amplification

CRISPR/Cas based biosensing systems have been demonstrated to have diagnostics capability with high specificity and super sensitivity (Qiu et al., 2018; Zuo et al., 2017), which is applicable to aptamer-based PADs. Recently we have summarised the CRISPR/Cas systems for biosensing applications (Li et al., 2019b). The use of paper lateral flow readout with CRISPR/Cas based biosensing systems has additionally realised the instrument free solution especially valuable for the POC scenarios. These systems have been evaluated for detection of various targets including bacteria, virus, cancer mutations, human genotype, SNPs differentiation et al. (Chertow, 2018; Gootenberg et al. 2017, 2018) Fig. 7 demonstrates a LFA based detection by using LwaCas13a enzyme from CRISPR-Cas13a family. CRISPR/Cas based system has the potential to significantly impact a variety of diagnostic fields by offering a much rapid and precise way for ultra-sensitive nucleic acid detection even to POC deployment with the similar simplicity for public to use that achieved by pregnant test strips. CRISPR/Cas based biosensing system is a completely new and potential diagnostic strategy, which will significantly impact PADs with superior signal amplification capability. We are expecting more exciting applications of CRISPR/Cas biosensing system based signal amplifications on PADs.

4. Engineering of PADs based signal amplification

Engineering architectures of PADs is another strategy to achieve signal amplification on PADs, it is mainly about applying surface modifications on paper surface (Rivas et al., 2014; Tang et al., 2017). Rivas et al. designed a sensitive AuNPs-based LFA strip by adding wax delay pillars (barriers) onto the nitrocellulose membrane to produce flow delays and pseudo turbulence in the flow (Fig. 8) providing a 3-fold highly sensitive result comparing with a conventional LFA (Rivas et al., 2014).

Integrating concentration technologies into paper LFA was also studied to enhance the sensitivity by using paper-based isotachophoresis to accelerate the surface reaction rate (Moghadam et al., 2015) or incorporating an aqueous two-phase system to concentrate biomarkers in samples (Chiu et al., 2014; Pereira et al., 2015). Tang et al. integrated a dialysis-based concentration method into LFAs by adding semi-permeable membrane, polyethylene glycol (PEG) and glass fiber, achieving a 10-fold signal enhancement of nucleic acid detection (HIV) and a 4-fold signal improvement of antigen detection (myoglobin) (Tang et al., 2016). Uniquely Kim's group used a water-swellable polymer to achieve an automatic switching LFIA to amplify the signal (Kim et al., 2016). A bridge membrane was integrated onto the conventional LFA strip with a reagent pad which had signal-enhancing materials or enzyme substrate. When the sample was added, the water-swellable polymer swelled and the reagent pad was able to attach to the test membrane. In this way, the secondary reagent was released from reagent pad to test membrane to generate or amplify the signal. By

I

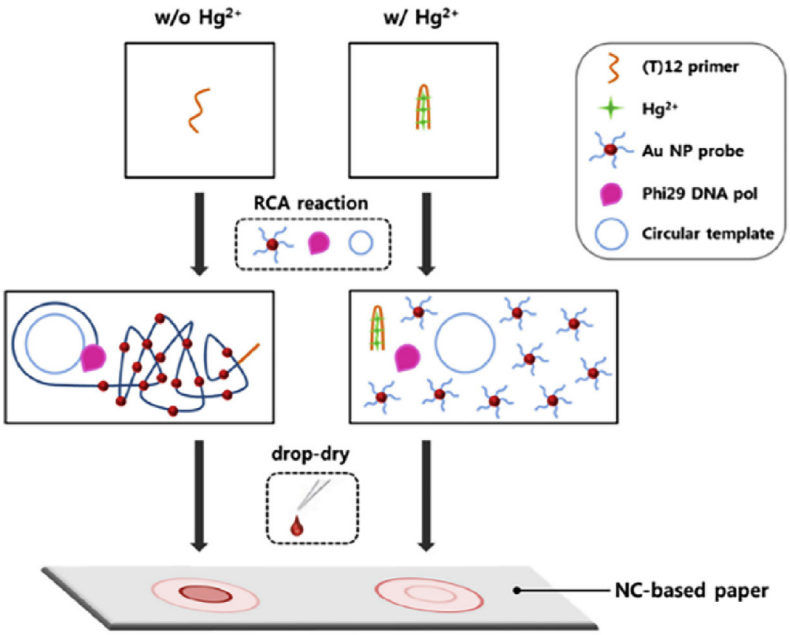

II

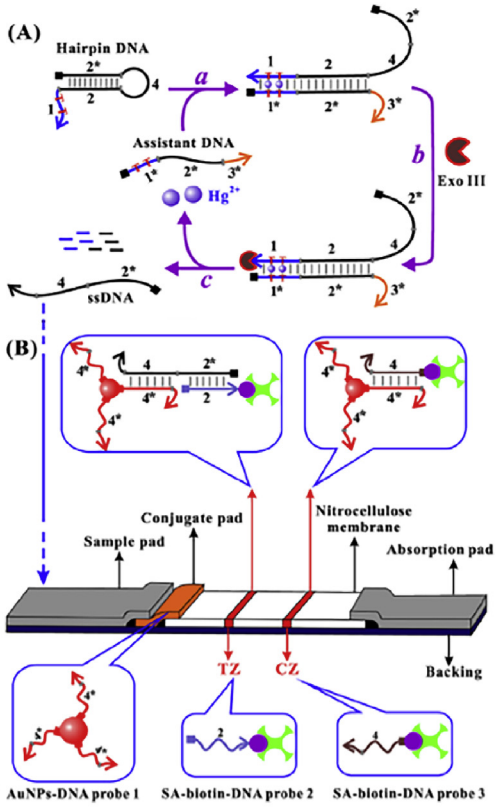

III

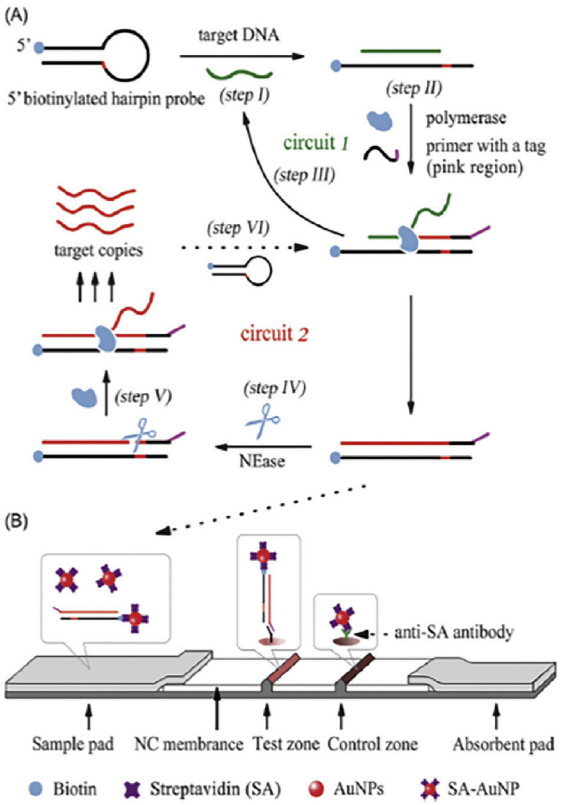

Fig. 6. For I: The schematics of the radial flow assay for Hg^{2+} detection using RCA and AuNPs probes for signal amplification. Reprinted with permission from (Kim et al., 2018a). For II: (A) The design scheme of Hg^{2+} detection. The numbers represent the domains while the asterisks represent the complementary of the related domains. Base pairs are represented by the short grey lines in the graph. The squares denote the 5′ termini while the arrows denote the 3′ termini of DNA strands. (B) The strip biosensor design. Reprinted with permission from (Chen et al., 2014). For III: (A) The schematic demonstration of the NASDP process and (B) the design of an LFA using NASDP method. Reprinted with permission from (Liu et al., 2013).

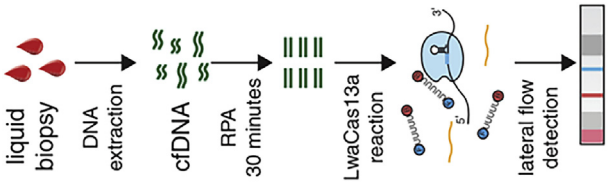

Fig. 7. Schematic detection of epidermal growth factor receptor (EGFR) mutations from patient liquid biopsy samples. Reprinted with permission from (Gootenberg et al., 2018).

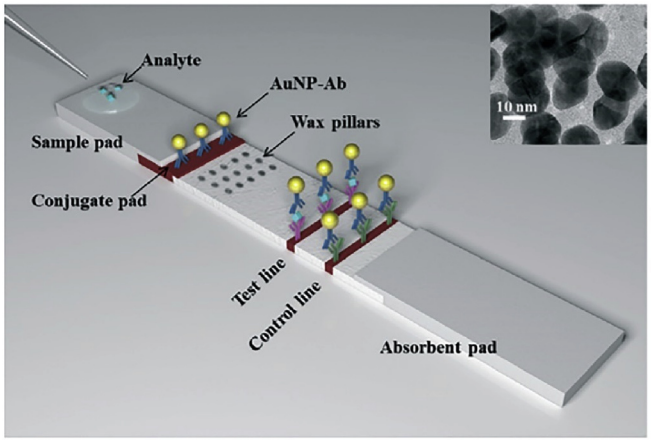

Fig. 8. The LFA strip with wax pillars added on the nitrocellulose membrane. Reprinted with permission from (Rivas et al., 2014).

using C-reactive protein as a model, the developed LFA strip provided a LOD as 0.03 ng/mL, which was lower than that of a conventional AuNPs-based LFA strip (13.65 ng/mL). This strategy can be combined with different chemical reaction-based assays, such as assays with metal-ion amplification, enzyme-catalyzed chemiluminescence assays *etc.* (Kim et al., 2016) Recently A simple and cost-effective nucleic acid hybridization-based LFA was designed for detection of hepatitis B virus by integrating sponge shunt onto the conjugation pad. The analytical sensitivity was improved 10-fold by the decreased fluid flow rate achieved by optimizing the thickness, hydrophobicity and length of the sponge (Tang et al., 2017).

Engineering the architecture of PADs such as controlling reagent transport on paper substrates by incorporating different materials, changing the shape and/or pore size of membranes and using concentration techniques provide a versatile, low-cost and relatively simple approach comparing with the nanotechnology based and nucleic acid based methods for enhancing signals. For example, the previously mentioned engineering method of using the wax printed barriers on the LFA strips can increase the sensitivity. However, the sensitivity enhancement and the related applications are limited due to the difficulty of flow rate control and the nature materials of PADs, also, alternating the shape or size of membranes will lead to the increase of sample volume needed. It is expected that the optimised signal amplification by combining the chemical methods with the engineering of PADs method will be applied in the future.

5. Conclusions and future directions

This review has discussed various strategies based on multiple technologies to increase the sensitivity of PADs. Advantages and disadvantages of these popular signal amplification strategies are summarised in Table 4.

AuNPs are the most popular nanomaterial used for signal amplification on PADs providing visible signal readout. Sensitivity will be further increased if AuNPs are integrated with other signal amplification strategies such as silver or gold enhancement, dual signal amplification, enzymes or catalytic metals. Besides AuNPs, QDs and graphene are commonly used for signal amplification on PADs. UCNPs provide a novel way of signal enhancement by providing strong and unique fluorescence signal while requiring specific laser detector. Also, natural enzymes combined with nanoparticles are able to provide enhanced signal, but this strategy has limitations regarding the preparation, purification and storage steps since natural enzymes are unstable and sensitive (Lan et al., 2016). While artificial enzymes on nanostructures provide a solution to the above-mentioned limitations and according to this, researchers used catalytic nanomaterials such as platinum nanoparticles coated on AuNPs on PADs for signal amplification.

Various isothermal nucleic acid amplification technologies (e.g., RCA, LAMP or RPA) (Loynachan et al., 2018) have been applied on PADs for sensitive analysis. Also, integrating both nucleic acid amplification and detection into one platform makes the detection simpler and cheaper (Choi et al., 2016a). However, there are still challenges associated with isothermal amplification methods normally requiring extra heating equipment, which is not cost-effective. In addition, complex enzymatic reactions and sophisticated assay designs further make the device less reproducible and robust (Liu et al., 2013). The recently discovered CRISPR/Cas system is another success to amplify signals for PADs with the sensitivity down from fM to aM (Chertow, 2018; Fu et al., 2016; Gootenberg et al. 2017, 2018; Myhrvold et al., 2018; Qiu et al., 2018; Zuo et al., 2017). With studies pushing deeper, CRISPR/Cas based systems have shown great potentials to become the most promising candidate of the next generation biosensing platforms for diagnostics with ultra-high specificity and superior sensitivity on PADs. Additionally, researchers are also interested in altering the PADs designs, for example, adding extra materials onto PADs to achieve a better performance (Tang et al., 2017).

To develop a sensitive and selective PAD system, signal amplification methods are crucial yet challenging for researchers. In view of future signal amplification strategies for PADs, incorporating novel technologies such as CRISPR/Cas biosensing system with new nanomaterials should be a promising and powerful direction. Applying fluidic control method into PAD system with simple fabrication and operation steps will be essential to increase the repeatability of PADs in POC diagnostics. We envision that the next generation of PAD systems will be simple, rapid, cost-effective, and multiplexed. They can provide accurate sensitive POC diagnostics which are detectable by naked eyes or by personal equipment such as smartphones towards the digital health monitoring. This will pave the way for PADs from bench to bedside with big success.

Conflicts of interest

There are no conflicts to declare.

Declaration of interests

The authors declare that they have no known competing financial interests or personal relationships that could have appeared to influence the work reported in this paper.

The authors declare the following financial interests/personal relationships which may be considered as potential competing interests:

Table 4
Summary of pros and cons of popular signal amplification strategies on PADs.

Signal Amplification Strategies	Description	Possible signal readout	Advantages	Disadvantages
Nanomaterials based	AuNPs; MNPs; QDs et al.	Colorimetric; Fluorescent; Chemiluminescent; Photoelectrochemical, SERS.	Versatile platforms; Low background noise for MNPs.	High cost; Complexity; Poor reproducibility.
Isothermal nucleic acid amplification techniques based	RCA; LAMP; SDA; RPA; HDA et al.	Colorimetric; Fluorescent.	Relatively high sensitivity and selectivity; Multiplex capability.	Complex assay designs with temperature control; Relative high cost; Long reaction time.
CRISPR/Cas based	Powerful nucleic-acid-sequence-based amplification.	Colorimetric; Fluorescent.	High specificity and sensitivity; Instrument free; Multiplex capability.	Further development of off-target effects required.
PADs designs based	Change the size of test strips or control the fluid flow.	Colorimetric; Chemiluminescent.	Economical and simple designs.	Limited sensitivity and applications.

CRediT authorship contribution statement

Linyang Liu: Writing - original draft, Writing - review & editing. **Danting Yang:** Writing - original draft, Writing - review & editing. **Guozhen Liu:** Conceptualization, Funding acquisition, Supervision, Project administration, Writing - review & editing.

Acknowledgements

This work was financially supported by the ARC Future Fellowship FT160100039, the ARC Centre of Excellence for Nanoscale BioPhotonics CE140100003, and the National Natural Science Foundation of China 21575045.

References

Akyazi, T., Basabe-Desmonts, L., Benito-Lopez, F., 2018. Anal. Chim. Acta 1001, 1–17.
Ali, M.M., Li, F., Zhang, Z., Zhang, K., Kang, D.K., Ankrum, J.A., Le, X.C., Zhao, W., 2014. Chem. Soc. Rev. 43 (10), 3324–3341.
Anfossi, L., Di Nardo, F., Giovannoli, C., Passini, C., Baggiani, C., 2013. Anal. Bioanal. Chem. 405 (30), 9859–9867.
Badu-Tawiah, A.K., Lathwal, S., Kaastrup, K., Al-Sayah, M., Christodouleas, D.C., Smith, B.S., Whitesides, G.M., Sikes, H.D., 2015. Lab Chip 15 (3), 655–659.
Bahadır, E.B., Sezgintürk, M.K., 2016. TrAC Trends Anal. Chem. (Reference Ed.) 82, 286–306.
Bu, T., Huang, Q., Yan, L., Huang, L., Zhang, M., Yang, Q., Yang, B., Wang, J., Zhang, D., 2018. Food Control 84, 536–543.
Burrs, S.L., Bhargava, M., Sidhu, R., Kiernan-Lewis, J., Gomes, C., Claussen, J.C., McLamore, E.S., 2016. Biosens. Bioelectron. 85, 479–487.
Cao, C., Zhang, F., Goldys, E.M., Gao, F., Liu, G., 2018. TrAC Trends Anal. Chem. (Reference Ed.) 102, 379–396.
Chao, C.C., Belinskaya, T., Zhang, Z., Ching, W.M., 2015. PLoS Neglected Trop. Dis. 9 (7), e0003884.
Chapman, R., Lin, Y., Burnapp, M., Bentham, A., Hillier, D., Zabron, A., Khan, S., Tyreman, M., Stevens, M.M., 2015. ACS Nano 9 (3), 2565–2573.
Chen, J., Zhou, S., Wen, J., 2014. Anal. Chem. 86 (6), 3108–3114.
Chen, M., Yang, H., Rong, L., Chen, X., 2016a. Analyst 141 (19), 5511–5519.
Chen, M., Yu, Z., Liu, D., Peng, T., Liu, K., Wang, S., Xiong, Y., Wei, H., Xu, H., Lai, W., 2015. Anal. Chim. Acta 876, 71–76.
Chen, X., Lan, J., Liu, Y., Li, L., Yan, L., Xia, Y., Wu, F., Li, C., Li, S., Chen, J., 2018a. Biosens. Bioelectron. 102, 582–588.
Chen, Y., Chen, Q., Han, M., Liu, J., Zhao, P., He, L., Zhang, Y., Niu, Y., Yang, W., Zhang, L., 2016b. Biosens. Bioelectron. 79, 430–434.
Chen, Y., Cheng, N., Xu, Y., Huang, K., Luo, Y., Xu, W., 2016c. Biosens. Bioelectron. 81, 317–323.
Chen, Y., Chu, W., Liu, W., Guo, X., Jin, Y., Li, B., 2018b. Microchim. Acta 185 (3), 187.
Chertow, D.S., 2018. Science 360 (6387), 381–382.
Chiu, R.Y., Jue, E., Yip, A.T., Berg, A.R., Wang, S.J., Kivnick, A.R., Nguyen, P.T., Kamei, D.T., 2014. Lab Chip 14 (16), 3021–3028.
Choi, J.R., Hu, J., Gong, Y., Feng, S., Wan Abas, W.A., Pingguan-Murphy, B., Xu, F., 2016a. Analyst 141 (10), 2930–2939.
Choi, J.R., Hu, J., Tang, R., Gong, Y., Feng, S., Ren, H., Wen, T., Li, X., Wan Abas, W.A.B., Pingguan-Murphy, B., Xu, F., 2016b. Lab Chip 16 (3), 611–621.
Choi, J.R., Yong, K.W., Tang, R., Gong, Y., Wen, T., Li, F., Pingguan-Murphy, B., Bai, D., Xu, F., 2017a. TrAC Trends Anal. Chem. (Reference Ed.) 93, 37–50.
Choi, S., Hwang, J., Lee, S., Lim, D.W., Joo, H., Choo, J., 2017b. Sens. Actuators, B 240, 358–364.
Connelly, J.T., Rolland, J.P., Whitesides, G.M., 2015. Anal. Chem. 87 (15), 7595–7601.
Cordray, M.S., Richards-Kortum, R.R., 2015. Malar. J. 14, 472.
Crannell, Z., Castellanos-Gonzalez, A., Nair, G., Mejia, R., White, A.C., Richards-Kortum, R., 2016. Anal. Chem. 88 (3), 1610–1616.
Craw, P., Balachandran, W., 2012. Lab Chip 12 (14).
Cunningham, J.C., DeGregory, P.R., Crooks, R.M., 2016. Annu. Rev. Anal. Chem. 9 (1), 183–202.
Deng, H., Liu, Q., Wang, X., Huang, R., Liu, H., Lin, Q., Zhou, X., Xing, D., 2017. Biosens. Bioelectron. 87, 931–940.
Deng, X., Wang, C., Gao, Y., Li, J., Wen, W., Zhang, X., Wang, S., 2018. Biosens. Bioelectron. 105, 211–217.
Duan, H., Huang, X., Shao, Y., Zheng, L., Guo, L., Xiong, Y., 2017. Anal. Chem. 89 (13), 7062–7068.
Fang, C.C., Chou, C.C., Yang, Y.Q., Wei-Kai, T., Wang, Y.T., Chan, Y.H., 2018. Anal. Chem. 90 (3), 2134–2140.
Feng, C., Mao, X., Shi, H., Bo, B., Chen, X., Chen, T., Zhu, X., Li, G., 2017. Anal. Chem. 89 (12), 6631–6636.
Fu, X., Cheng, Z., Yu, J., Choo, P., Chen, L., Choo, J., 2016. Biosens. Bioelectron. 78, 530–537.
Gao, X., Zheng, P., Kasani, S., Wu, S., Yang, F., Lewis, S., Nayeem, S., Engler-Chiurazzi, E.B., Wigginton, J.G., Simpkins, J.W., 2017a. Anal. Chem. 89 (18), 10104–10110.
Gao, Z., Ye, H., Tang, D., Tao, J., Habibi, S., Minerick, A., Tang, D., Xia, X., 2017b. Nano Lett. 17 (9), 5572–5579.
Ge, S., Li, W., Yan, M., Song, X., Yu, J., 2015. J. Mater. Chem. B 3 (12), 2426–2432.
Ghosh, D.K., Kokane, S.B., Kokane, A.D., Warghane, A.J., Motghare, M.R., Bhose, S., Sharma, A.K., Reddy, M.K., 2018. PLoS One 13 (12), e0208530.
Gootenberg, J.S., Abudayyeh, O.O., Kellner, M.J., Joung, J., Collins, J.J., Zhang, F., 2018. Science 360 (6387), 439–444.
Gootenberg, J.S., Abudayyeh, O.O., Lee, J.W., Essletzbichler, P., Dy, A.J., Joung, J., Verdine, V., Donghia, N., Daringer, N.M., Freije, C.A., 2017. Science 356 (6336), 438–442.
Hasanzadeh, M., Shadjou, N., 2016. Mater. Sci. Eng. C 61, 979–1001.
Hasanzadeh, M., Shadjou, N., de la Guardia, M., 2015. TrAC Trends Anal. Chem. (Reference Ed.) 72, 1–9.
He, M., Li, Z., Ge, Y., Liu, Z., 2016. Anal. Chem. 88 (3), 1530–1534.
Hu, J., Huang, R., Sun, Y., Wei, X., Wang, Y., Jiang, C., Geng, Y., Sun, X., Jing, J., Gao, H., 2019. J. Microbiol. Methods 158, 25–32.
Hu, J., Jiang, Y.Z., Wu, L.L., Wu, Z., Bi, Y., Wong, G., Qiu, X., Chen, J., Pang, D.W., Zhang, Z.L., 2017. Anal. Chem. 89 (24), 13105–13111.
Hu, J., Wang, S., Wang, L., Li, F., Pingguan-Murphy, B., Lu, T.J., Xu, F., 2014. Biosens. Bioelectron. 54, 585–597.
Hu, J., Zhang, Z.L., Wen, C.Y., Tang, M., Wu, L.L., Liu, C., Zhu, L., Pang, D.W., 2016. Anal. Chem. 88 (12), 6577–6584.
Huang, K.J., Shuai, H.L., Zhang, J.Z., 2016a. Biosens. Bioelectron. 77, 69–75.
Huang, X., Aguilar, Z.P., Xu, H., Lai, W., Xiong, Y., 2016b. Biosens. Bioelectron. 75, 166–180.
Hui, C.Y., Liu, M., Li, Y., Brennan, J.D., 2018. Angew. Chem. Int. Ed. 57 (17), 4549–4553.
Hwang, J., Lee, S., Choo, J., 2016. Nanoscale 8 (22), 11418–11425.
Jaroenram, W., Owens, L., 2014. J. Virol. Methods 208, 144–151.
Jauset-Rubio, M., Svobodova, M., Mairal, T., McNeil, C., Keegan, N., El-Shahawi, M.S., Bashammakh, A.S., Alyoubi, A.O., O'Sullivan, C.K., 2016a. Anal. Chem. 88 (21), 10701–10709.
Jauset-Rubio, M., Svobodova, M., Mairal, T., McNeil, C., Keegan, N., Saeed, A., Abbas, M.N., El-Shahawi, M.S., Bashammakh, A.S., Alyoubi, A.O., CK, O.S., 2016b. Sci. Rep. 6, 37732.
Jiang, T., Song, Y., Du, D., Liu, X., Lin, Y., 2016. ACS Sens. 1 (6), 717–724.
Jin, B., Wang, S., Lin, M., Jin, Y., Zhang, S., Cui, X., Gong, Y., Li, A., Xu, F., Lu, T.J., 2017. Biosens. Bioelectron. 90, 525–533.
Kaarj, K., Akarapipad, P., Yoon, J.Y., 2018. Sci. Rep. 8 (1), 12438.
Kersting, S., Rausch, V., Bier, F.F., von Nickisch-Rosenegk, M., 2014. Malar. J. 13 (1), 99.
Kim, K., Joung, H.A., Han, G.R., Kim, M.G., 2016. Biosens. Bioelectron. 85, 422–428.
Kim, T.Y., Lim, M.C., Woo, M.A., Jun, B.H., 2018a. Nanomaterials 8 (2), 81.
Kim, W., Lee, S., Jeon, S., 2018b. Sens. Actuators, B 273, 1323–1327.
Koczula, K.M., Gallotta, A., 2016. Essays Biochem. 60 (1), 111–120.
Lamas-Ardisana, P.J., Casuso, P., Fernandez-Gauna, I., Martínez-Paredes, G., Jubete, E., Añorga, L., Cabañero, G., Grande, H.J., 2017. Electrochem. Commun. 75, 25–28.
Lan, F., Sun, G., Liang, L., Ge, S., Yan, M., Yu, J., 2016. Biosens. Bioelectron. 79, 416–422.
Lathwal, S., Sikes, H.D., 2016. Lab Chip 16 (8), 1374–1382.

Leem, H., Shukla, S., Song, X., Heu, S., Kim, M., 2014. J. Food Saf. 34 (3), 239–248.
Li, F., Zhang, H., Wang, Z., Newbigging, A.M., Reid, M.S., Li, X.F., Le, X.C., 2015. Anal. Chem. 87 (1), 274–292.
Li, G., Xu, L., Wang, D., Jiang, J., Chen, X., Zhang, W., Poapolathep, S., Poapolathep, A., Zhang, Z., Zhang, Q., 2018. Anal. Chem. 91 (3), 1968–1973.
Li, J., Duan, H., Xu, P., Huang, X., Xiong, Y., 2016. RSC Adv. 6 (31), 26178–26185.
Li, J., Macdonald, J., 2015. Biosens. Bioelectron. 64, 196–211.
Li, L., Li, W., Yang, H., Ma, C., Yu, J., Yan, M., Song, X., 2014a. Electrochim. Acta 120, 102–109.
Li, L., Ma, C., Kong, Q., Li, W., Zhang, Y., Ge, S., Yan, M., Yu, J., 2014b. J. Mater. Chem. B 2 (38), 6669–6674.
Li, L., Xu, J., Zheng, X., Ma, C., Song, X., Ge, S., Yu, J., Yan, M., 2014c. Biosens. Bioelectron. 61, 76–82.
Li, T.-T., Wang, J.-L., Zhang, N.-Z., Li, W.-H., Yan, H.-B., Li, L., Jia, W.-Z., Fu, B.-Q., 2019a. Fron. Cell. Infect. Microbiol. 9, 1.
Li, W., Li, L., Ge, S., Song, X., Ge, L., Yan, M., Yu, J., 2014d. Biosens. Bioelectron. 56, 167–173.
Li, X., Li, W., Yang, Q., Gong, X., Guo, W., Dong, C., Liu, J., Xuan, L., Chang, J., 2014e. ACS Appl. Mater. Interfaces 6 (9), 6406–6414.
Li, Y., Li, S., Wang, J., Liu, G., 2019b. Trends Biotechnol (in press).
Liang, L., Su, M., Li, L., Lan, F., Yang, G., Ge, S., Yu, J., Song, X., 2016. Sens. Actuators, B 229, 347–354.
Liang, Z., Wang, X., Zhu, W., Zhang, P., Yang, Y., Sun, C., Zhang, J., Wang, X., Xu, Z., Zhao, Y., Yang, R., Zhao, S., Zhou, L., 2017. ACS Appl. Mater. Interfaces 9 (4), 3497–3504.
Lin, L.-K., Stanciu, L.A., 2018. Sens. Actuators, B 276, 222–229.
Linnes, J.C., Fan, A., Rodriguez, N.M., Lemieux, B., Kong, H., Klapperich, C.M., 2015. RSC Adv. 5 (77) 62585-62585.
Linnes, J.C., Rodriguez, N.M., Liu, L., Klapperich, C.M., 2016. Biomed. Microdevices 18 (2), 30.
Liu, F., Ge, S., Yu, J., Yan, M., Song, X., 2014a. Chem. Commun. 50 (71), 10315–10318.
Liu, F., Zhang, H., Wu, Z., Dong, H., Zhou, L., Yang, D., Ge, Y., Jia, C., Liu, H., Jin, Q., Zhao, J., Zhang, Q., Mao, H., 2016a. Talanta 161, 205–210.
Liu, H., Crooks, R.M., 2011. J. Am. Chem. Soc. 133 (44), 17564–17566.
Liu, H., Xiang, Y., Lu, Y., Crooks, R.M., 2012. Angew. Chem. 51 (28), 6925–6928.
Liu, J., Chen, L., Lie, P., Dun, B., Zeng, L., 2013. Chem. Commun. 49 (45), 5165–5167.
Liu, M., Hui, C.Y., Zhang, Q., Gu, J., Kannan, B., Jahanshahi-Anbuhi, S., Filipe, C.D., Brennan, J.D., Li, Y., 2016b. Angew. Chem. Int. Ed. 55 (8), 2709–2713.
Liu, R., Zhang, Y., Zhang, S., Qiu, W., Gao, Y., 2014b. Appl. Spectrosc. Rev. 49 (2), 121–138.
Liu, W., Ma, C., Yang, H., Zhang, Y., Yan, M., Ge, S., Yu, J., Song, X., 2014c. Microchim. Acta 181 (11–12), 1415–1422.
Liu, W.J., Yang, Y.T., Du, S.M., Yi, H.D., Xu, D.N., Cao, N., Jiang, D.L., Huang, Y.M., Tian, Y.B., 2019. J. Virol. Methods 266, 34–40.
Loynachan, C.N., Thomas, M.R., Gray, E.R., Richards, D.A., Kim, J., Miller, B.S., Brookes, J.C., Agarwal, S., Chudasama, V., McKendry, R.A., Stevens, M.M., 2018. ACS Nano 12 (1), 279–288.
Luo, Q., Wang, L.V., Tuchin, V.V., Liu, H., Xing, D., Zhou, X., 2014. Point of Care Nucleic Acid Detection of Viable Pathogenic Bacteria with Isothermal RNA Amplification Based Paper Biosensor. Twelfth International Conference on Photonics and Imaging in Biology and Medicine. PIBM 2014.
Ma, C., Li, W., Kong, Q., Yang, H., Bian, Z., Song, X., Yu, J., Yan, M., 2015. Biosens. Bioelectron. 63, 7–13.
Magro, L., Escadafal, C., Garneret, P., Jacquelin, B., Kwasiborski, A., Manuguerra, J.C., Monti, F., Sakuntabhai, A., Vanhomwegen, J., Lafaye, P., Tabeling, P., 2017. Lab Chip 17 (14), 2347–2371.
Mahato, K., Srivastava, A., Chandra, P., 2017. Biosens. Bioelectron. 96, 246–259.
Malekzad, H., Zangabad, P.S., Mirshekari, H., Karimi, M., Hamblin, M.R., 2017. Nanotechnol. Rev. 6 (3), 301–329.
Martinez, A.W., Phillips, S.T., Butte, M.J., Whitesides, G.M., 2007. Angew. Chem. Int. Ed. 46 (8), 1318–1320.
Moghadam, B.Y., Connelly, K.T., Posner, J.D., 2015. Anal. Chem. 87 (2), 1009–1017.
Mohammed, L., Gomaa, H.G., Ragab, D., Zhu, J., 2017. Particuology 30, 1–14.
Morales-Narvaez, E., Naghdi, T., Zor, E., Merkoci, A., 2015. Anal. Chem. 87 (16), 8573–8577.
Myhrvold, C., Freije, C.A., Gootenberg, J.S., Abudayyeh, O.O., Metsky, H.C., Durbin, A.F., Kellner, M.J., Tan, A.L., Paul, L.M., Parham, L.A., 2018. Science 360 (6387), 444–448.
Notomi, T., Okayama, H., Masubuchi, H., Yonekawa, T., Watanabe, K., Amino, N., Hase, T., 2000. Nucleic Acids Res. 28 (12) e63-e63.
Oliveira-Rodriguez, M., Serrano-Pertierra, E., Garcia, A.C., Lopez-Martin, S., Yanez-Mo, M., Cernuda-Morollon, E., Blanco-Lopez, M.C., 2017. Biosens. Bioelectron. 87, 38–45.
Omidfar, K., Kia, S., Kashanian, S., Paknejad, M., Besharatie, A., Kashanian, S., Larijani, B., 2010. Appl. Biochem. Biotechnol. 160 (3), 843–855.
Ouyang, S., Zhang, Z., He, T., Li, P., Zhang, Q., Chen, X., Wang, D., Li, H., Tang, X., Zhang, W., 2017. Toxins 9 (4), 137.
Panferov, V.G., Safenkova, I.V., Varitsev, Y.A., Zherdev, A.V., Dzantiev, B.B., 2017. Microchim. Acta 185 (1), 25.
Park, H.J., Yang, S.C., Choo, J., 2016a. Bull. Korean Chem. Soc. 37 (12), 2019–2024.
Park, J.-M., Jung, H.-W., Chang, Y.W., Kim, H.-S., Kang, M.-J., Pyun, J.-C., 2015. Anal. Chim. Acta 853, 360–367.
Park, J., Shin, J.H., Park, J.-K., 2016b. Anal. Chem. 88 (7), 3781–3788.
Parolo, C., de la Escosura-Muniz, A., Merkoci, A., 2013. Biosens. Bioelectron. 40 (1), 412–416.
Parolo, C., Merkoci, A., 2013. Chem. Soc. Rev. 42 (2), 450–457.
Peeling, R.W., Mabey, D., 2010. Clin. Microbiol. Infect. 16 (8), 1062–1069.
Peng, X., Kang, L., Pang, F., Li, H., Luo, R., Luo, X., Sun, F., 2018. Food Agric. Immunol. 29 (1), 216–227.
Pereira, D.Y., Chiu, R.Y., Zhang, S.C., Wu, B.M., Kamei, D.T., 2015. Anal. Chim. Acta 882, 83–89.
Phillips, E.A., Moehling, T.J., Bhadra, S., Ellington, A.D., Linnes, J.C., 2018. Anal. Chem. 90 (11), 6580–6586.
PRNewswire, 2018. Global Point-of-Care/Rapid Diagnostics Market (2018-2022) Forecast to Grow at a CAGR of 10% - High Prevalence of Infectious Diseases in Developing Countries. https://www.prnewswire.com/news-releases/global-point-of-carerapid-diagnostics-market-2018-2022-forecast-to-grow-at-a-cagr-of-10—high-prevalence-of-infectious-diseases-in-developing-countries-300629579.html April 2019.
Qiu, W., Xu, H., Takalkar, S., Gurung, A.S., Liu, B., Zheng, Y., Guo, Z., Baloda, M., Baryeh, K., Liu, G., 2015. Biosens. Bioelectron. 64, 367–372.
Qiu, X.Y., Zhu, L.Y., Zhu, C.S., Ma, J.X., Hou, T., Wu, X.M., Xie, S.S., Min, L., Tan, D.A., Zhang, D.Y., Zhu, L., 2018. ACS Synth. Biol. 7 (3), 807–813.
Qiu, Z., Shu, J., Tang, D., 2017. Anal. Chem. 89 (9), 5152–5160.
Quesada-Gonzalez, D., Merkoci, A., 2015. Biosens. Bioelectron. 73, 47–63.
Ratnarathorn, N., Chailapakul, O., Henry, C.S., Dungchai, W., 2012. Talanta 99, 552–557.
Razo, S.C., Panferov, V.G., Safenkova, I.V., Varitsev, Y.A., Zherdev, A.V., Dzantiev, B.B., 2018. Anal. Chim. Acta 1007, 50–60.
Reid, M.S., Le, X.C., Zhang, H., 2018. Angew. Chem. Int. Ed. 57 (37), 11856–11866.
Ren, M., Xu, H., Huang, X., Kuang, M., Xiong, Y., Xu, H., Xu, Y., Chen, H., Wang, A., 2014. ACS Appl. Mater. Interfaces 6 (16), 14215–14222.
Ren, W., Cho, I.H., Zhou, Z., Irudayaraj, J., 2016. Chem. Commun. 52 (27), 4930–4933.
Rivas, L., Medina-Sánchez, M., de la Escosura-Muñiz, A., Merkoçi, A., 2014. Lab Chip 14 (22), 4406–4414.
Rivas, L., Reutersward, P., Rasti, R., Herrmann, B., Martensson, A., Alfven, T., Gantelius, J., Andersson-Svahn, H., 2018. Talanta 183, 192–200.
Rodriguez, M.O., Covian, L.B., Garcia, A.C., Blanco-Lopez, M.C., 2016. Talanta 148, 272–278.
Rodriguez, N.M., Linnes, J.C., Fan, A., Ellenson, C.K., Pollock, N.R., Klapperich, C.M., 2015. Anal. Chem. 87 (15), 7872–7879.
Rohrman, B., Richards-Kortum, R., 2015. Anal. Chem. 87 (3), 1963–1967.
Rong, Z., Xiao, R., Xing, S., Xiong, G., Yu, Z., Wang, L., Jia, X., Wang, K., Cong, Y., Wang, S., 2018. Analyst 143 (9), 2115–2121.
Roskos, K., Hickerson, A.I., Lu, H.W., Ferguson, T.M., Shinde, D.N., Klaue, Y., Niemz, A., 2013. PLoS One 8 (7), e69355.
Sajid, M., Kawde, A.-N., Daud, M., 2015. J. Saudi Chem. Soc. 19 (6), 689–705.
Sánchez-Purrà, M., Roig-Solvas, B., Versiani, A., Rodriguez-Quijada, C., de Puig, H., Bosch, I., Gehrke, L., Hamad-Schifferli, K., 2017. Mol. Syst. Des. Eng. 2 (4), 401–409.
Sapountzi, E.A., Tragoulias, S.S., Kalogianni, D.P., Ioannou, P.C., Christopoulos, T.K., 2015. Anal. Chim. Acta 864, 48–54.
Scida, K., Cunningham, J.C., Renault, C., Richards, I., Crooks, R.M., 2014. Anal. Chem. 86 (13), 6501–6507.
Seok, Y., Joung, H.-A., Byun, J.-Y., Jeon, H.-S., Shin, S.J., Kim, S., Shin, Y.-B., Han, H.S., Kim, M.-G., 2017. Theranostics 7 (8), 2220–2230.
Shao, Y., Duan, H., Guo, L., Leng, Y., Lai, W., Xiong, Y., 2018. Anal. Chim. Acta 1025, 163–171.
Sharma, S., Zapatero-Rodriguez, J., Estrela, P., O'Kennedy, R., 2015. Biosensors 5 (3), 577–601.
Shen, H., Xu, F., Xiao, M., Fu, Q., Cheng, Z., Zhang, S., Huang, C., Tang, Y., 2017. Analyst 142 (23), 4393–4398.
Shetty, P., Ghosh, D., Singh, M., Tripathi, A., Paul, D., 2016. RSC Adv. 6 (61), 56205–56212.
Shi, Q., Huang, J., Sun, Y., Deng, R., Teng, M., Li, Q., Yang, Y., Hu, X., Zhang, Z., Zhang, G., 2018. Microchim. Acta 185 (2), 84.
Sun, G., Ding, Y.-n., Ma, C., Zhang, Y., Ge, S., Yu, J., Song, X., 2014. Electrochim. Acta 147, 650–656.
Syedmoradi, L., Daneshpour, M., Alvandipour, M., Gomez, F.A., Hajghassem, H., Omidfar, K., 2017. Biosens. Bioelectron. 87, 373–387.
Tang, R., Yang, H., Choi, J.R., Gong, Y., Hu, J., Feng, S., Pingguan-Murphy, B., Mei, Q., Xu, F., 2016. Talanta 152, 269–276.
Tang, R., Yang, H., Gong, Y., Liu, Z., Li, X., Wen, T., Qu, Z., Zhang, S., Mei, Q., Xu, F., 2017. Sci. Rep. 7 (1), 1360.
Taranova, N.A., Berlina, A.N., Zherdev, A.V., Dzantiev, B.B., 2015. Biosens. Bioelectron. 63, 255–261.
Tian, T., Bi, Y., Xu, X., Zhu, Z., Yang, C., 2018. Anal. Methods 10 (29), 3567–3581.
Wang, D., Zhang, Z., Li, P., Zhang, Q., Zhang, W., 2016a. Sensors 16 (7), 1094.
Wang, M., Hou, W., Mi, C.-C., Wang, W.-X., Xu, Z.-R., Teng, H.-H., Mao, C.-B., Xu, S.-K., 2009. Anal. Chem. 81 (21), 8783–8789.
Wang, R., Kim, K., Choi, N., Wang, X., Lee, J., Jeon, J.H., Rhie, G.-e., Choo, J., 2018. Sens. Actuators, B 270, 72–79.
Wang, S., Ge, L., Yan, M., Yu, J., Song, X., Ge, S., Huang, J., 2013a. Sens. Actuators, B 176, 1–8.
Wang, X., Choi, N., Cheng, Z., Ko, J., Chen, L., Choo, J., 2017. Anal. Chem. 89 (2), 1163–1169.
Wang, Y., Ge, L., Wang, P., Yan, M., Ge, S., Li, N., Yu, J., Huang, J., 2013b. Lab Chip 13 (19), 3945–3955.
Wang, Y., Liu, H., Wang, P., Yu, J., Ge, S., Yan, M., 2015. Sens. Actuators, B 208, 546–553.
Wang, Y., Xu, H., Luo, J., Liu, J., Wang, L., Fan, Y., Yan, S., Yang, Y., Cai, X., 2016b. Biosens. Bioelectron. 83, 319–326.
Wiriyachaiporn, N., Maneeprakorn, W., Apiwat, C., Dharakul, T., 2014. Microchim. Acta 182 (1–2), 85–93.
Wu, L., Ma, C., Ge, L., Kong, Q., Yan, M., Ge, S., Yu, J., 2015a. Biosens. Bioelectron. 63, 450–457.

Wu, L., Ma, C., Zheng, X., Liu, H., Yu, J., 2015b. Biosens. Bioelectron. 68, 413–420.
Wu, M.Y., Hsu, M.Y., Chen, S.J., Hwang, D.K., Yen, T.H., Cheng, C.M., 2017. Trends Biotechnol. 35 (4), 288–300.
Wu, Y., Xue, P., Hui, K.M., Kang, Y., 2014a. ChemElectroChem 1 (4), 722–727.
Wu, Y., Xue, P., Hui, K.M., Kang, Y., 2014b. Biosens. Bioelectron. 52, 180–187.
Wu, Y., Xue, P., Kang, Y., Hui, K.M., 2013. Anal. Chem. 85 (18), 8661–8668.
Xia, S., Yu, Z., Liu, D., Xu, C., Lai, W., 2016a. Food Control 59, 507–512.
Xia, Y., Si, J., Li, Z., 2016b. Biosens. Bioelectron. 77, 774–789.
Xiao, K., Wang, K., Qin, W., Hou, Y., Lu, W., Xu, H., Wo, Y., Cui, D., 2017. Talanta 164, 463–469.
Xiao, W., Huang, C., Xu, F., Yan, J., Bian, H., Fu, Q., Xie, K., Wang, L., Tang, Y., 2018. Sens. Actuators, B 266, 63–70.
Xu, G., Nolder, D., Reboud, J., Oguike, M.C., van Schalkwyk, D.A., Sutherland, C.J., Cooper, J.M., 2016. Angew. Chem. 55 (49), 15250–15253.
Xu, H., Chen, J., Birrenkott, J., Zhao, J.X., Takalkar, S., Baryeh, K., Liu, G., 2014. Anal. Chem. 86 (15), 7351–7359.
Yamada, K., Henares, T.G., Suzuki, K., Citterio, D., 2015. Angew. Chem. Int. Ed. 54 (18), 5294–5310.
Yamada, K., Shibata, H., Suzuki, K., Citterio, D., 2017. Lab Chip 17 (7), 1206–1249.
Yan, L., Dou, L., Bu, T., Huang, Q., Wang, R., Yang, Q., Huang, L., Wang, J., Zhang, D., 2018. Food Chem. 261, 131–138.
Yang, W., Ratinac, K.R., Ringer, S.P., Thordarson, P., Gooding, J.J., Braet, F., 2010. Angew. Chem. Int. Ed. 49 (12), 2114–2138.
Yao, L., Teng, J., Zhu, M., Zheng, L., Zhong, Y., Liu, G., Xue, F., Chen, W., 2016. Biosens. Bioelectron. 85, 331–336.
Ye, H., Xia, X., 2018. J. Mater. Chem. B 6 (44), 7102–7111.
Yen, C.W., de Puig, H., Tam, J.O., Gomez-Marquez, J., Bosch, I., Hamad-Schifferli, K., Gehrke, L., 2015. Lab Chip 15 (7), 1638–1641.
Yetisen, A.K., Akram, M.S., Lowe, C.R., 2013. Lab Chip 13 (12), 2210–2251.
You, M., Lin, M., Gong, Y., Wang, S., Li, A., Ji, L., Zhao, H., Ling, K., Wen, T., Huang, Y., Gao, D., Ma, Q., Wang, T., Ma, A., Li, X., Xu, F., 2017. ACS Nano 11 (6), 6261–6270.
Yu, L., Shi, Z.Z., 2015. Lab Chip 15 (7), 1642–1645.
Yu, Q., Li, H., Li, C., Zhang, S., Shen, J., Wang, Z., 2015. Food Control 54, 347–352.
Zangheri, M., Cevenini, L., Anfossi, L., Baggiani, C., Simoni, P., Di Nardo, F., Roda, A., 2015. Biosens. Bioelectron. 64, 63–68.
Zeng, F., Duan, W., Zhu, B., Mu, T., Zhu, L., Guo, J., Ma, X., 2018. Anal. Chem. 91 (1), 1064–1070.
Zhan, L., Guo, S.-z., Song, F., Gong, Y., Xu, F., Boulware, D.R., McAlpine, M.C., Chan, W.C., Bischof, J.C., 2017. Nano Lett. 17 (12), 7207–7212.
Zhang, D., Huang, L., Liu, B., Ni, H., Sun, L., Su, E., Chen, H., Gu, Z., Zhao, X., 2018. Biosens. Bioelectron. 106, 204–211.
Zhang, X., Yu, X., Wen, K., Li, C., Mujtaba Mari, G., Jiang, H., Shi, W., Shen, J., Wang, Z., 2017. J. Agric. Food Chem. 65 (36), 8063–8071.
Zhao, M., Li, H., Liu, W., Chu, W., Chen, Y., 2017. Sens. Actuators, B 242, 87–94.
Zhao, M., Wang, B., Xiang, L., Xiong, C., Shi, Y., Wu, L., Meng, X., Dong, G., Xie, Y., Sun, W., 2019. Food Control 100, 117–121.
Zhao, W., Ali, M.M., Brook, M.A., Li, Y., 2008. Angew. Chem. Int. Ed. 47 (34), 6330–6337.
Zhao, Y., Liu, X., Wang, X., Sun, C., Wang, X., Zhang, P., Qiu, J., Yang, R., Zhou, L., 2016. Talanta 161, 297–303.
Zhong, Y., Chen, Y., Yao, L., Zhao, D., Zheng, L., Liu, G., Ye, Y., Chen, W., 2016. Microchim. Acta 183 (6), 1989–1994.
Zuo, X., Fan, C., Chen, H.-Y., 2017. Nat. Biomed. Eng. 1 (6) 0091.